DOMAIN BRIDGING INTERACTIONS IN THE ALLOSTERIC NETWORK FOR IIA^{GLC} INHIBITION OF THE *ESCHERICHIA COLI* GLYCEROL KINASE

A Thesis

by

EDITH ABENA ACQUAYE

Submitted to the Office of Graduate Studies of
Texas A&M University
in partial fulfillment of the requirements for the degree of

MASTER OF SCIENCE

August 2010

Major Subject: Biochemistry

Domain Bridging Interactions in the Allosteric Network for IIA^{Glc} Inhibition of the *Escherichia coli* Glycerol Kinase

DOMAIN BRIDGING INTERACTIONS IN THE ALLOSTERIC NETWORK FOR IIA^{GLC} INHIBITION OF THE *ESCHERICHIA COLI* GLYCEROL KINASE

A Thesis

by

EDITH ABENA ACQUAYE

Submitted to the Office of Graduate Studies of
Texas A&M University
in partial fulfillment of the requirements for the degree of

MASTER OF SCIENCE

Approved by:

Chair of Committee,	Donald W. Pettigrew
Committee Members,	Mary Bryk
	Frank Raushel
Head of Department,	Gregory Reinhart

August 2010

Major Subject: Biochemistry

ABSTRACT

Domain Bridging Interactions in the Allosteric Network for IIA^{Glc} Inhibition of the *Escherichia coli* Glycerol Kinase. (August 2010)

Edith Abena Acquaye, B.Sc., University of Ghana

Chair of Advisory Committee: Dr. Donald W. Pettigrew

Previous studies on inhibition of the *Escherichia coli* glycerol kinase enzyme have suggested that subunit-subunit or domain bridging interactions form part of the network in communicating ligand binding to inhibition. In this study, five amino acids were identified to be in close proximity to an Arg^{369} residue which is a domain bridging residue. Three of the amino acid residues (Q37, Y39 and Q104) are in domain I of the enzyme subunit, while the other two (M308 and Q314) are in domain II of the enzyme subunit.

To evaluate the importance of each domain bridging residue in IIA^{Glc} inhibition, alanine substitutions were made of the residues, and the kinetic properties characterized with respect to IIA^{Glc} inhibition. Kinetic parameters obtained for each variant glycerol kinase enzyme was compared to values obtained for the Wild Type enzyme to assess the importance of the amino acid residue in IIA^{Glc} inhibition. The effects of the substitutions on FBP inhibition as well as catalysis of the enzyme were also analyzed by obtaining kinetic parameters for each of the variant enzymes.

The results from this study indicate that the domain I bridging interactions with Arg^{369} are important in IIA^{Glc} regulation of the *E. coli* glycerol kinase enzyme. The domain II bridging interactions appear to be unimportant in regulating IIA^{Glc} inhibition. Two of the domain I bridging residues studied were also found to be important in FBP inhibition. These results indicate that some the domain bridging residues seen to be involved in IIA^{Glc} regulation also appear to be involved in FBP regulation. In catalysis, with the exception of Q314, the rest of the domain I and II bridging residues appear to be important for substrate binding and/or catalysis.

DEDICATION

I dedicate this thesis to my husband, Dan Seedah, my parents, Mr and Mrs Acquaye, and my sister, Ellen Acquaye. Their encouragement has been a pillar of strength for me.

ACKNOWLEDGEMENTS

I thank my committee chair and research supervisor, Dr. Pettigrew for his guidance, support, and patience throughout the course of this research. His support has been instrumental throughout the program. I also thank my committee members Dr. Mary Bryk and Dr. Frank Raushel for their advice, time and support. Thanks to Pamela S. Miller for her technical help and to Damien Terry and Shanna Mayorov for their help with the determination of some of the kinetic parameters.

I also thank all my friends and colleagues and the department faculty and staff for making my time at Texas A&M University a great experience.

Finally, thanks to my parents for their encouragement and to my husband for his patience and love.

TABLE OF CONTENTS

CHAPTER Page

LIST OF FIGURES

FIGURE Page

LIST OF TABLES

CHAPTER I

INTRODUCTION

Under low glucose conditions, glycerol can be metabolized to provide energy in *E. coli*. Studies of glycerol metabolism have revealed two modes of glycerol dissimilation in bacteria. In the first mode, glycerol may be oxidized to dihydroxyacetone (DHA), and then phosphorylated to dihydroxyacetone phosphate (DHAP), while in the second method, glycerol is phosphorylated to glycerol-3-phosphate (G3P), and then oxidized to DHAP. Both routes however result in the terminal product DHAP which enters the glycolytic pathway to provide energy for the organism (1). The enzymes involved in the preliminary steps of glycerol dissimilation are outlined below.

Mode A:

Enzyme 1: Glycerol dehydrogenase (EC 1 . 1 . 1 .6; Glycerol:NAD^+ 2-oxidoreductase):

Reaction 1: Glycerol + $NAD^+ \leftrightarrow$ DHA + NADH + H^+

Enzyme 2: DHA kinase (EC 2 . 7 . 1 .28: Triokinase)

Reaction 2: DHA + ATP $\rightarrow$ DHAP + ADP

This thesis follows the style of the *Journal of Biological Chemistry*.

1. The abbreviations used are: IIA^{Glc}, enzyme of the PTS which is specific for glucose; βME, 2-mercaptoethanol; DHA, dihydroxyacetone; DHAP, dihydroxyacetone phosphate; FBP, fructose-1,6-bisphosphate; G3P, glycerol-3-phosphate; glp, glycerol phosphate regulon; IPTG, isopropylthiogalactoside; n_H, Hill Coefficient; MGSA, MacConkey glycerol plates containing streptomycin and ampicillin; PTS, phosphoenolpyruvate:glycose phosphotransferase system; SDS, sodium dodecyl sulfate; TEA, triethanolamide; single and three letter abbreviations are used for amino acids.

Mode B:

Enzyme 1: Glycerol kinase (EC 2 .7. 1 .30; ATP:glycerol 3-phosphotransferase):

Reaction 1: Glycerol + ATP → G3P + ADP

Enzyme 2: Glycerol-3-phosphate dehydrogenase (EC 1 . 1 . 1 .8; sn-Glycerol-3-phosphate:NAD^+ 2-oxidoreductase)

Reaction 2: G3P → DHAP

The phosphorylation of glycerol to glycerol-3-phosphate by the enzyme glycerol kinase has been found to be a key regulatory step in glycerol metabolism (1, 2). The EcGK is encoded by the *glpK* gene whose transcription is upregulated with other genes needed for glycerol metabolism (3, 4). The crystal structure of EcGK shows that it is a member of the sugar kinase kinase/actin/heat shock protein 70 (hsp 70) superfamily of proteins (5). These proteins are characterized by two large domains, I and II, one on either side of a deep narrow ATPase catalytic cleft (6, 7, 8). As with other sugar kinases, ligand binding to the EcGK is presumed to affect closure of the catalytic site cleft due to movement of one domain relative to the other (9, 10, 11). The catalytic activity of EcGK has been found to be activated by ATP which displays apparent two classes of binding sites, glycerol, (12) and by interaction with the glycerol facilitator (13). The Michaelis constants have been found to be 10-fold less than the substrate dissociation constants, suggesting that some step after the formation of the ternary complexes may be at least partially rate limiting (12).

When glycerol is not needed as a carbon source, the activity of EcGK is allosterically regulated by the glycolytic intermediate fructose-1,6-bisphosphate (FBP)

(14), and the glucose-specific phosphocarrier protein of the phosphoenolpyruvate:glycose phosphostransferase system, IIA^{Glc} (15). Regulation of EcGK by FBP is by feedback inhibition and has been found to display characteristics of a V system (14). EcGK exists in a dimer-tetramer equilibrium with the dimer being the active form and the tetramer being the inactive form. FBP binding has been shown to shift the equilibrium strongly towards the tetramer therefore effecting inhibition (16). In contrast, regulation by IIA^{Glc} has been found to be via protein-protein interactions (5, 17, 18). IIA^{Glc} may be phosphorylated on the active site His^{90} which is the prevalent form of IIA^{Glc} when extracellular glucose is not available (18). Unphosphorylated IIA^{Glc} is thus the form which inhibits EcGK when glucose is available. The two allosteric inhibitors, FBP and IIA^{Glc}, bind at distances of 35 Å and 30 Å, respectively, from the enzyme catalytic site (5). FBP binds only in domain I while IIA^{Glc} binds only in domain II, raising the question of how the perturbations due to ligand binding at separate regions of the enzyme are propagated to the distant catalytic site in this oligomeric protein to result in inhibition. It is thought that the regulation of EcGK by the two allosteric inhibitors IIA^{Glc} and FBP are independent of each other and can be genetically separated (18, 19).

Analysis of the x-ray crystallographic structure of the *E. coli* glycerol kinase (EcGK) has not offered a complete insight into the allosteric inhibition of the enzyme. The structural basis for the allosteric control of EcGK appears different from that of the other members of the superfamily that EcGK belongs to (20). For most of the other superfamily members, including hexokinases, actin, and hsp 70, their crystal structures show that their allosteric effectors interact with both domains and it is generally believed

that the effectors act directly on the cleft closure (20). For these superfamily members, it appears that their allosteric regulation is as a result of direct steric action on the cleft closure due the interactions of the allosteric effectors with both domains. In EcGK however, the mechanism of allosteric regulation by IIA^{Glc} and FBP does not appear to be due to direct steric action on the catalytic site closure because each allosteric effector is found to bind in only one domain.

Current views on allosteric control of proteins have expanded on the classical view of allostery (21, 22). In the classical view, regulation of protein function by allosteric effectors was thought to be due to conformational changes that reflect global cooperativity within the protein (23, 24). Recent studies of the allosteric control of proteins however indicate that allosteric behavior may occur as a result of changes in local interactions among a few amino acid residues (25, 26, 27, 28). These amino acids are thought to form networks for long-range energetic interactions in proteins (25). Previous studies of EcGK suggest that subunit-subunit/domain interactions of the *E. coli* glycerol kinase enzyme may be important for ligand binding of its allosteric inhibitors and subsequent inhibition. Such interactions may form part of the network for the allosteric control of EcGK; this would be in agreement with the current views of allosteric control of proteins.

In 1993, Hurley et al. (5) suggested that the amino residue, Arg^{369}, may be involved in the allosteric regulation of glycerol kinase. They reached this conclusion from analysis of the crystal structure of the glycerol kinase enzyme with the substrates ADP and glycerol, which showed Arg^{369} as present on a loop from one subunit which

penetrates deeply, approaching approximately 7 Å of the ADP molecule in the next subunit. Recent studies by Pettigrew (20) agreed with the hypothesis of Hurley et al. (5) by showing that truncation of the Arg^{369} residue with an R369A mutation resulted in a reduction of the inhibition of glycerol kinase by one of its allosteric inhibitors IIA^{Glc}. The results also showed that inhibition by the other allosteric inhibitor FBP was not affected by the R369A substitution. Liu et al. in 1994 (29) also showed that an A65T mutation in glycerol kinase resulted in abolishing inhibition of glycerol kinase by FBP. Analysis of the crystal structure of the enzyme showed that this mutation is associated with an α-helix that constitutes one of the two subunit-subunit interfaces within the tetramer. These observations support the premise that the domain interactions of the Arg^{369} residue of the *E. coli* glycerol kinase enzyme may be important in the network of amino acid residues which communicate changes due to IIA^{Glc} binding in the allosteric regulation of the enzyme.

The crystal structure of EcGK shows that the Arg^{369} side chain from one subunit interacts with both domains of the other subunit. A close inspection of the domain bridging interactions shows three amino acids in domain I (Q37, Y39, Q104) with side chains within 3.5Å of the guanidino group of Arg^{369} and two amino acids in domain II (M308, Q314) with side chains within 4.8 Å of the guanidino group of Arg^{369}. In this study, amino acid substitutions were therefore made for the five amino acid residues identified within 7 Å of the residue Arg^{369} to assess the contribution of the hydrogen bonding interactions between the side chains of the amino acids residues and the guanidino group of the Arg^{369} in the regulation of the enzyme by IIA^{Glc}. The inhibition

parameters obtained were then compared to the Wild Type enzyme. Kinetic parameters were also obtained from measuring the extent of inhibition of the variant enzymes by FBP. The contribution of each domain interaction with Arg^{369} in the catalytic activity of the enzyme was determined from comparing the catalytic kinetic parameters obtained for the Wild Type and variant glycerol kinase enzymes.

Some of the recent studies on the contributions of individual amino acids in enzyme catalysis and regulation use NMR spectroscopy as a useful tool because it is sensitive to molecular motion over a wide variety of timescales. The subunit size of the tetrameric EcGK is approximately 56 kD, which exceeds the protein NMR size limit of 35 kD (30), therefore preventing the use of NMR to investigate the role of specific amino acid residues in EcGK. Structure perturbation studies have however proved to be a powerful alternative approach in studies of protein regulation. The effects of changes in the regulatory properties of the protein due to specific changes in the primary structure of the protein can be analyzed.

In this study, structure perturbation was used to study the five amino acids identified in close proximity to Arg^{369}. Amino acid substitutions were made and the effects of the mutations assessed by using kinetics to characterize the regulatory properties. The following specific aims were used to address the objective of understanding the role and contribution of the domain bridging interactions in the regulation of EcGK by IIA^{Glc}.

Specific Aims

1. Construction and purification of glycerol kinase variants with amino acid substitutions of the residues flanking the Arg^{369} residue.
2. Characterization of the IIA^{Glc} regulatory properties as well as the catalytic properties and regulation by FBP of the variant glycerol kinase enzymes.
3. Evaluation of the contribution of each domain interaction with Arg^{369}.

CHAPTER II

MATERIALS AND METHODS

Materials

Chemicals and enzymes were purchased from Sigma-Aldrich Chemical Co. (St. Louis, Mo.) unless otherwise stated. The enzyme IIA^{Glc} used in this study was purified from pVEX-crr plasmids expressing the IIA^{Glc} encoding sequence and purified from the BL21 (DE3) strain of *E. coli* bearing the plasmid as described (31). The pVEX-crr plasmid was generously provided by Dr. Saul Roseman, Department of Biology, Johns Hopkins University (Baltimore, MD). SDS electrophoresis reagents were purchased from Fisher. Plasmid purification kits were purchased from Qiagen Sciences (Valencia, CA). The QuikChange™ site directed mutagenesis method was used for the purposes of this study

Strains and Plasmids

The strain of *E. coli* used in this study was the K12 DG1 (genotype: F^- ara *glpR208 Δ(lac-proAB) rpL* (Str^r) [Φ80dlac*Δ*(lacZ)M15] *thi glpK202*) strain, which is streptomycin resistant and ampicillin sensitive. This strain of *E. coli* was constructed in the Pettigrew laboratory to provide a glycerol kinase deletion background for mutagenesis work. The pWT165 plasmid vector contains the Wild Type glycerol kinase gene and confers ampicillin resistance for positive selection of transformed cells. The pWT165 plasmid was previously constructed by cloning the *Hind* III fragment that

contains the glycerol kinase gene from the rfMl3 DNA that was used in the sequencing of the gene (32) into the vector pHG165 (33). Single mutations were introduced in the glycerol kinase encoding sequences by using the QuikChange™ site directed mutagenesis method for the purposes of this study.

Mutant Plasmid DNA Construction

Single mutations were introduced in the glycerol kinase encoding sequences by using the QuikChange™ site directed mutagenesis method. Table 1 shows the sites of the single amino acid substitutions that were made in the glycerol kinase coding sequence. Amino acid residues in domain I and II which are in close proximity to the Arg^{369} residue were substituted with alanine. One amino acid residue in domain I, Y39, was also substituted with phenylalanine to assess the contribution of the hydroxyl group interaction of the tyrosine residue with Arg^{369}.

Table 1: Sites of single amino acid substitutions introduced into the glycerol kinase sequence

Domain I substitutions	Domain II substitutions
Q37A	M308A
Y39A	Q314A
Q104A	
Y39F	

The native sequences below contain the sites for introducing the single mutations into the glycerol kinase encoding sequence. The desired sites for substitutions are underlined. The variant sequences with the desired mutations were used as primers for the site directed mutagenesis. For the alanine substitutions, the mutation site codon was changed to GCG (a codon for alanine) in primer 1 and CGC (anticodon) in primer 2. For the Y39F substitution however, the mutation site codon was changed to TTT (a codon for phenylalanine) in primer 1 and AAA (anticodon) in primer 2.

Q37A

PRIMER 1: 5' - CAG CGC GAA TTT GAG CAA ATC TAC CCA AAA CCA - 3'

PRIMER 2: 5' - TGG TTT TGG GTA GAT TTG CTC AAA TTC GCG CTG - 3'

Y39A

PRIMER 1: 5'- GAA TTT GAG CAA ATC TAC CCA AAA CCA GGT TGG - 3'

PRIMER 2: 5'- CCA ACC TGG TTT TGG GTA GAT TTG CTC AAA TTC - 3'

Y39F

PRIMER 1: 5' - GAA TTT GAG CAA ATC TTT CCA AAA CCA GGT TGG - 3'

PRIMER 2: 5'- CCA ACC TGG TTT TGG AAA GAT TTG CTC AAA TTC - 3'

Q104A

PRIMER 1: 5’ - AAC GCC ATT GTC TGG CAG TGC CGT CGT ACC GCA - 3’
PRIMER 2: 5’- TGC GGT ACG ACG GCA CTG CCA GAC AAT GGC GTT - 3’

M308A

PRIMER 1: 5’ - GAA GGT GCG GTG TTT ATG GCA GGC GCA TCC ATT - 3’

PRIMER 2: 5’- AAT GGA TGC GCC TGC CAT AAA CAC CGC ACC TTC - 3’

Q314A

PRIMER 1: 5’- GCA GGC GCA TCC ATT CAG TGG CTG CGC GAT GAA - 3’

PRIMER 2: 5’ - TTC ATC GCG CAG CCA CTG AAT GGA TGC GCC TGC - 3’

The mutant strands were generated by PCR thermocycling using the conditions outlined below:

1. 94^{o}C for 1 minute
2. 94^{o}C for 30 seconds
3. 59.8^{o}C for 30 seconds
4. 68^{o}C for 20 minutes

   Repeat steps 2 to 4 for 15 cycles
5. 68^{o}C for 10 minutes
6. 4^{o}C - Hold

Transformation of *E. coli* and Verification of Mutant Plasmids

The transformation of *E. coli* with the appropriate mutant plasmid was done by the calcium chloride method (34). Cells successfully transformed with the mutant plasmids were screened on MacConkey-glycerol plates containing ampicillin and streptomycin sulfate (MGSA plates). Cells containing the glpK gene in pWT165 plasmid are pink to purple on MacConkey glycerol agar depending on their ability to metabolize glycerol. The antibiotics ampicillin and streptomycin sulfate where indicated were added to final concentrations of 75µg/ml and 200µg/ml respectively. Transformants were then streaked on MGSA and single colonies picked and grown in 1X LB broth containing ampicillin and streptomycin sulfate (LBSA). Plasmid DNA was then purified from the cell cultures using the Qiagen™ miniprep DNA purification kit. The purified plasmid DNA was sequenced and verified for incorporation of the desired amino acid substitution in the glycerol kinase gene. The primers used for sequencing the glycerol kinase sequence are written out in Table 2. The plasmid DNA from each glycerol kinase variant was sequenced using the ABI Big Dye method. The reactions were performed by using a reaction mix containing 400-600ng of speed vacuum dried purified DNA, 1µl of a 10µM stock of each primer, 2µl of ABI Big Dye (a polymerase, dideoxynucleotides mix),and 3µl sterile milliQ water. The thermocycling conditions for the sequencing reaction were as follows:

1. 95^{o}C for 2 minutes
2. 95 ^{o}C for 30 seconds
3. 50 ^{o}C 15 seconds

4. 60 ^{o}C 4 minutes

   Repeat steps 2 to 4 for 99 cylces

5. 4 ^{o}C - Hold

The PCR products were cleaned by gel filtration using spin columns provided by the Gene Technologies Laboratory, Department of Biology, TAMU. The cleaned products of the sequencing reactions DNA were air dried in a SpeedVac and analyzed by the Gene Technologies Laboratory, Department of Biology, TAMU. The sequences obtained were then verified for correct incorporation of the desired single mutation by comparing each sequence to the Wild Type glycerol kinase sequence using the Sequencher® 4.1.4 software.

Table 2: Primer sequences used for amplification and sequencing of the glycerol kinase gene

PRIMER NAME	SEQUENCE	GC CONTENT	Tm
DP 1	TGGCGAAAGCCGATATCAGTT	47.6	56.8
DP 2	GTGGAAGGCTCTCGCGAGCGT	66.7	64.3
DP 3	GGCAAAGGCGGCACGCGTATT	61.9	63.7
DP 4	TGGCTGCGCGATGAAATGAAG	52.4	58.7
DP 5	GGCCGACTCTGGTATCCGTCT	61.9	60.7
DP 6	TACCGTTACGCAGGCTGGAAA	52.4	58.8
P 1	GACACGCTAATGATATTGGCA	42.9	53.0
P 2	AATGCTCGCAGATTTCTGCGG	52.4	58.5
P 3	AACAGCAATTCACCACGACGT	47.6	57.5
P 4	CAGTGCCATAGGTGTTCTTCG	52.4	55.8
P 5	CGGAATCGTAGGCGTCGTTAA	52.4	57.0
P 6	TCGGACTGGAACTGCATCAGG	57.1	59.2

Enzyme Purification

The variant glycerol kinase enzymes (Q37A, Y39A, Y39F, Q104A, M308A, and Q314A) were expressed and purified as described by Pettigrew et al., (35) with the following modifications: The enzyme was expressed from the pWT165 plasmid and not the pCJ102 plasmid. The transformed cells were grown in cultures containing both ampicillin and streptomycin. The purification procedure involved usage of a GE Pharmacia ATKA™ purifier system.

Overexpression of Enzyme

The *E. coli* cells containing the variant glycerol kinases were grown in 1 L of 2X LB broth containing streptomycin and ampicillin. Each culture was grown in a 37^{o}C shaker overnight. The next day, the overnight culture was induced for three hours with IPTG at a concentration of 1 mM. The resulting cell cultures were spun at 6,000 rpm at 4^{o}C for 10 minutes, in a Sorvall RC5-B refrigerated super-speed centrifuge using a GS3 rotor. The harvested cells were stored at -20^{o}C until used.

Cell Lysis

Before cell lysis, the cells were resuspended in four volumes of glpK standard buffer pH 8.0 composed of 50 mM TEA, 2 mM glycerol, 1 mM EDTA and 2 mM βME (12). A W-220F sonicator with a microtip (Heat systems – Ultrasonics, Inc) was used to lyse the cells. The cells were sonicated for 10 minutes using 2 seconds sonication/3 seconds off cycling, in a salt ice-bath, with the temperature of the cell suspension maintained below 10^{o}C. The resulting cell suspension was centrifuged at 12,000 rpm in a FiberLite F15S-8X50C rotor and the supernatant tested for activity.

Enzyme Purification

The supernatant from the cell lysis was taken through steps of addition of streptomycin sulfate and ammonium sulfate to precipitate out nucleic acids and finally the glycerol kinase proteins. The streptomycin and ammonium sulfate steps were carried out in the cold unless indicated otherwise. The enzymes were purified using the AKTA purifier system which combines Q-Sepharose HP and Source 15Q affinity chromatography systems. Each enzyme was stored as a crystalline ammonium sulfate suspension as described (35).

Streptomycin Sulfate Treatment

To precipitate nucleic acids, 20% streptomycin sulfate in glpK standard buffer pH 8.0 was added slowly to the crude supernatant while stirring continuously. The volume of the 20% streptomycin sulfate prepared and added was $1/10^{th}$ the volume of the crude supernatant. The mixture was stirred for an additional 30 minutes and then centrifuged for 10 minutes in the FiberLite F15S-8X50C rotor at 12,000 rpm. The supernatant volume was measured, labeled SSR and an aliquot assayed for activity. The pellet was stored at 4^{o}C.

Ammonium Sulfate Treatment

The streptomycin sulfate treated supernatant was taken through two ammonium sulfate treatments to first precipitate out unwanted proteins and then to precipitate out the EcGK. In the first ammonium sulfate treatment, finely ground ammonium sulfate (24g/100 mL SSR) was slowly added with constant stirring. The stirring was continued for an additional 30 minutes in the cold room after which the solution was centrifuged

for 10 minutes in the FiberLite F15S-8X50C rotor at 12,000 rpm. The supernatant volume was measured, labeled ASSI and an aliquot assayed for activity. The resulting pellet was stored at 4^{o}C. The ASSI was then taken through the second ammonium sulfate treatment by adding 22g/ 100 mL ASSI of finely ground ammonium sulfate while stirring continuously. The stirring was continued for an additional 30 minutes and the mixture centrifuged for 10 minutes in the FiberLite F15S-8X50C rotor at 12,000 rpm. The supernatant was labeled ASSIIsupe and the volume measured. The ASSIIsupe was assayed to make sure no activity was left in the ammonium sulfate fraction. The pellet was then resuspended in standard buffer pH 8.0 (1/10th the volume of the ASSIIsupe), and dialyzed overnight versus 1 L of standard buffer pH 8.0 and labeled ASSIIpptd. The ASSIIpptd was assayed for activity the next day.

Column Purification

The proteins were then purified using the AKTA^{TM} purifier system which combined Q-Sepharose HP and Source 15Q affinity chromatography systems. The ASSIIpptd was first centrifuged at 12,000 rpm for 10 minutes in the FiberLite F15S-8X50C rotor and then syringe filtered with the Millipore filter (0.45 μM). The protein was then run on the Q-Sepharose HP column (approximately 2.6 cm x 11.8 cm) with standard buffer pH 8.0 and eluted with 10-50% NaCl in standard buffer pH 8.0. Enzyme containing fractions as determined by assaying for enzyme activity were pooled. The Q-Sepharose HP pool was then dialyzed against 1 L of standard buffer pH 7.0 and assayed for activity. The Q-Sepharose HP pool was centrifuged at 12,000 rpm for 10 minutes in the FiberLite F15S-8X50C rotor; syringe filtered and then run through the first Source

15Q column at pH 7.0 (approximately 1.5 cm x 11.2 cm); the column was then eluted with a 10-50% NaCl in standard buffer pH 8.0. Enzyme containing fractions were pooled and dialyzed against 1 L of standard buffer pH 8.0. The Source 15Q pH 7.0 pool was then centrifuged at 12,000 rpm for 10 minutes in the FiberLite F15S-8X50C rotor; syringe filtered and then run through the second Source 15Q column at pH 8.0 and eluted with 10-50% NaCl gradient. The protein concentrations and enzyme activity of enzyme containing fractions were determined from the absorbance at 280nm on a Beckman UV/Vis DU800 spectrophotometer using an extinction coefficient of 1.73 $(mg/mL)^{-1}cm^{-1}$ (36), and by assaying for enzyme activity respectively. Homogeneity of the purified glycerol kinase enzyme was then determined using SDS-PAGE with GelCode Blue stain, and pure fractions pooled. The purified proteins were dialyzed against standard buffer pH 8.0 and concentrated by ultrafiltration using the 30 000 kD molecular weight cut-off Centricon® centrifugal filter device. Each enzyme was stored as a crystalline ammonium sulfate suspension as described (35).

Preparation of Purified Enzyme for Initial Velocity Studies and Inhibition Assays

Before each experiment, each enzyme was passed through a NAP-10 mini-column. The mini-column was first washed with three column volumes of standard buffer, pH 7.0 to equilibrate the column. A volume of the enzyme diluted in standard buffer, pH 7.0 and made up to 1 mL was loaded onto the equilibrated mini-column and the flow-through discarded. A volume of 1.4 mL of standard buffer, pH 7.0 was then loaded unto the mini-column and the flow-through collected for protein concentration and subsequent enzyme activity analysis. This served to remove the ammonium sulfate

that the enzymes were stored in. The concentration of the enzyme after passing through the mini-column was determined from the absorbance at 280nm on a Beckman UV/Vis DU800 spectrophotometer using an extinction coefficient of 1.73 $(mg/mL)^{-1}cm^{-1}$ (36).

Enzyme Assays

IIA^{Glc} Inhibition Studies

IIA^{Glc} inhibition of the enzyme activity of the glycerol kinase variants was measured in the forward reaction (glycerol to glycerol-3-phosphate) using the continuous ADP-coupled spectrophotometric assay at pH 7.0 and 25°C with a Beckman DU800 spectrophotometer. The enzyme inhibition assay is composed of a 0.5 mL solution of 50mM triethanolamine-HCl buffer, 5 mM $MgCl_2$, 20 mM KCl, 7.5 units each of pyruvate kinase and lactate dehydrogenase, 0.2 mM PEP, 0.2 mM NADH, 10 mM glycerol and 2.5 mM ATP with varying concentrations of IIA^{Glc} from 0- 60 μM. The assay was initiated by the addition of the enzyme. Data were fit to equation 1 below using the Kaleidagraph software (Synergy Software, Reading, PA). The glycerol kinase enzyme concentration in each assay was varied from 0.5 to 5 μg/ml, depending on the activity of the variant enzyme. For each of the variant enzymes, the inhibition parameter $K_{0.5}$ which is the apparent dissociation constant for allosteric effector binding was determined from the fits of the data to equation 1.

$$SA_{[X]} = SA_o - \frac{(SA_o - SA_\infty)[X]}{K_{0.5} + [X]} \quad (1)$$

- X is the allosteric inhibitor IIA^{Glc},

- $SA_{[X]}$ is the specific activity at the concentration of the inhibitor,
- SA_0 is the specific activity in the absence of the inhibitor,
- SA_∞ is the specific activity in the saturating presence of inhibitor,
- $K_{0.5}$ is equal to the concentration of X that gives 50% of the maximum inhibition.

Another inhibition parameter, W, is the coupling parameter which describes the effect of the allosteric ligand on V_{max} and was determined from equation 2 below.

$$W = \frac{SA_\infty}{SA_o} \quad (2)$$

where SA_∞ – SA at saturating levels of the inhibitor

SA_o – SA in the absence of the inhibitor

The value of W is >1 if the allosteric effector increases the V_{max}, and is <1 if V_{max} is reduced by the allosteric effector. Where there is no allosteric effect on V_{max}, W equals 1.

FBP Inhibition Studies

The FBP inhibition assay also had the same components of the IIA^{Glc} inhibition assay except FBP concentrations were varied from 0- 10 mM. Also, the reaction assay was incubated with the enzyme and FBP for 90 minutes before initiating the reaction by the addition of ATP. Data were fit to the equation 3 below using the Kaleidagraph software (Synergy Software, Reading, PA).

$$SA_{[X]} = SA_o - \frac{(SA_o - SA_\infty)[X]^{nH}}{(K_{0.5})nH + [X]^{nH}} \quad (3)$$

- X is the allosteric inhibitor FBP,
- $SA_{[X]}$ is the specific activity at the concentration of the inhibitor,
- SA_0 is the specific activity in the absence of the inhibitor,
- SA_∞ is the specific activity in the saturating presence of inhibitor,
- $K_{0.5}$ is equal to the concentration of *X* that gives 50% of the maximum inhibition,
- n_H is the Hill Coefficient and describes the binding cooperativity of the allosteric effector.

The glycerol kinase enzyme concentration in the FBP assays was varied from 0.5 to 5 μg/ml, depending on the activity of the variant enzyme. For each of the variant enzymes, the inhibition parameter $K_{0.5}$ which is the apparent dissociation constant for allosteric effector binding was determined from the fits of the data to equation 3. The coupling parameter W, for FBP inhibition was determined from equation 2.

Enzyme Catalytic Activity Assays

The assays to assess the catalytic activity of the variant enzymes had the same components of the inhibition assays except the substrate ATP was varied from 0 - 2.5 mM and no inhibitor was added to the assays. Wild Type EcGK has been shown to display two classes of ATP binding sites (12). The determination of kinetic parameters is more accurate for the first ATP binding site. ATP concentrations were therefore varied from 0 – 0.1 mM to obtain the kinetic parameters for assessing the catalytic properties.

For variants where the substitutions appeared to decrease the ATP binding affinity , the ATP concentrations were varied up to 2.5 mM. Kinetic data was fit to the Michaelis-Menten equation 4 below using the Kaleidagraph software (Synergy Software, Reading, PA).

$$v_o = \frac{V_{max}[ATP]}{[ATP] + K_m^{ATP}} \qquad (4)$$

where the catalytic activity of the enzymes with respect to the substrate glycerol was assessed, glycerol concentration was varied from 0 – 1.6 mM, while ATP was varied from 0 – 2.5 mM. Kinetic data was fit to equation 5 below for a bi-substrate enzyme kinetics mechanism using the program EnzFitter (Biosoft, Cambridge, U.K.). The concentration of glycerol kinase enzyme used in the enzyme assays varied from 0.5 to 5 μg/ml, depending on the activity of the variant enzyme.

$$v_o = \frac{V\,max[ATP][gol]}{[ATP][gol] + K_m^{ATP}[gol] + K_m^{gol}[ATP] + K_{ia}^{ATP}K_m^{gol}} \qquad (5)$$

- v_o is the intial velocity at the concentration of substrate,
- V_{max} is the maximum velocity at saturating conditions of the substrate,
- [ATP] is the concentration of ATP,
- K_m^{ATP} is the Michaelis constant for ATP,
- [gol] is the concentration of glycerol,
- K_{ia}^{ATP} is the dissociation constant for ATP,
- K_m^{gol} is the Michaelis constant for glycerol.

IIA^{Glc} Binding Studies

Sedimentation velocity experiments were used to assess IIA^{Glc} binding to EcGK as described (37). Purified glycerol kinase protein samples were diluted to 0.3 mg/mL of glycerol kinase with standard buffer, pH 7.0. The IIA^{Glc} concentration was varied from 0 up to 90 μM. Samples were run in a Beckman model XL-A analytical ultracentrifuge at 28,500 rpm and 25°C. Scans were performed at 280 nm with 4 minute intervals between scans. The data obtained were analyzed using the SVEDBERG program (version 6.38) to obtain the apparent sedimentation coefficient. The dissociation constant for IIA^{Glc} binding to glycerol kinase was determined by fitting the IIA^{Glc} concentration dependence of the apparent sedimentation coefficients (S_{app}) to equation 6.

$$S_{app} = S_o + (S_\infty - S_o)\left(\frac{[GK * IIA^{Glc}]}{[GK]_{TOT}}\right) \quad (6)$$

where,

$$[GK * IIA^{Glc}] = \frac{\left([GK]_{TOT} + [IIA^{Glc}]_{TOT} + K_d\right) - \left(([GK]_{TOT} + [IIA^{Glc}]_{TOT} + K_d)^2 - 4[GK]_{TOT}[IIA^{Glc}]_{TOT}\right)^{\frac{1}{2}}}{2}$$

- S_o is the sedimentation coefficient in the absence of IIA^{Glc},
- S_∞ is the sedimentation coefficient in the saturating presence of IIA^{Glc},
- S_{app} is the apparent sedimentation coefficient,
- $[GK]_{TOT}$ is the concentration of total enzyme,
- $[IIA^{Glc}]_{TOT}$ is the concentration of total IIA^{Glc},
- K_d is the dissociation constant.

CHAPTER III

RESULTS

Construction and Purification of Variant Glycerol Kinases

E. coli cells transformed with the products of the mutagenized DNA were selected on MGSA plates. Five to ten pink to purple colonies indicative of glycerol utilization were selected for sequencing to identify the mutants. Plasmid DNA purified from the *E. coli* cells which were sequenced confirmed at least one selected colony with the desired single mutations introduced into the glycerol kinase gene with no secondary mutations.

The variant glycerol kinase enzymes Q37A, Y39A, Y39F, Q104A, M308A and Q314A were purified as outlined in the materials and methods section. During the purification steps, ammonium sulfate solubility of the variant enzymes was comparable to that of the Wild Type and to each other. Elution positions on the Q-Sepharose and Source 15Q chromatography columns were similar, suggesting that the structure of the enzyme was not grossly altered by the mutations incorporated. Each enzyme was purified as shown in the SDS-PAGE gel image (Figure 1). However, the specific activity after the final purification step of each variant enzyme varied. Wild Type glycerol kinase was found to have a specific activity of approximately 39 U/mg. Q37A, Y39F, Q104A and Q314A had specific activities comparable to Wild Type. There was however a 20-fold reduction in the specific activity of Y39A and a 2-3 fold reduction in specific activity of M308A compared to the Wild Type.

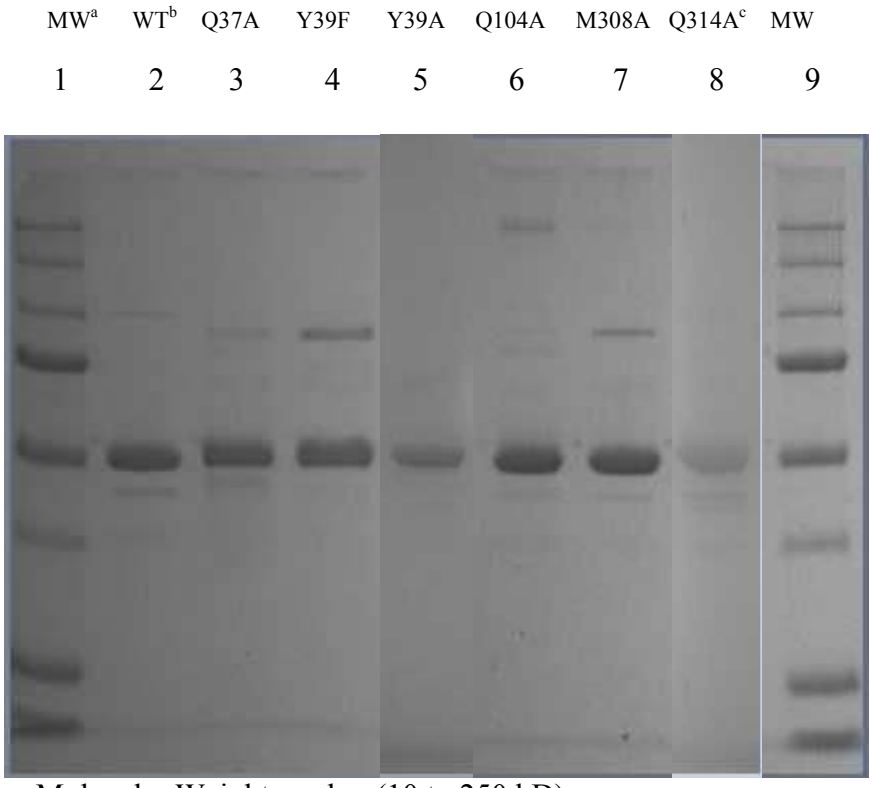

a: Molecular Weight marker (10 to 250 kD)
b: Wild Type glycerol kinase – purified by Pamela Miller
c: Q314A variant – purified by Damien Terry

Figure 1: SDS-PAGE of purified variant glycerol kinase proteins. For each well, 5 µg of protein was loaded. This gel picture is a composite of two separate gels. Wells 1 to 4, 6, 7 and 9 are from one gel while wells 5 and 8 are from a different gel.

IIA^{Glc} Inhibition of Wild Type and Glycerol Kinase Variants

Figures 2-7 show the IIA^{Glc} inhibition of the Wild Type and alanine variant enzymes. The figure on page 35 shows the IIA^{Glc} inhibition of the phenylalanine variant. Each of the alanine variants was inhibited by IIA^{Glc} except for the Y39A variant, for which no inhibition was detected. The parameters $K_{0.5}$ for IIA^{Glc} inhibition were determined from fitting the dependence of the specific activity of the Wild Type and variant glycerol kinases on IIA^{Glc} concentration to equation 1 while W was determined from equation 2. The kinetic constants determined from the IIA^{Glc} inhibition studies displayed in Table 3 are the average values of the kinetic constants determined from at least two independent experiments.

The $K_{0.5}$ for IIA^{Glc} binding to Wild Type glycerol kinase was found to be 4.6 μM. This value compares to what has been previously determined (29). Considering the domain I variants, there was a slight increase in the $K_{0.5}$ value for the domain I Q37 alanine variant. For the domain I variant Y39A, the $K_{0.5}$ value was not determined because no inhibition was observed.

To assess the relative role of the tyrosine hydroxyl group and the aromatic ring in the loss of IIA^{Glc} inhibition of the Y39A variant, the Y39F variant was constructed. The dependence of its catalytic activity on IIA^{Glc} concentration shows it is inhibited by IIA^{Glc}. The IIA^{Glc} inhibition parameters for the Y39F variant are shown in Table 3. The $K_{0.5}$ and W were not significantly different from the values obtained for Wild Type EcGK. Considering the domain II variants, the $K_{0.5}$ was not significantly different from the Wild Type.

The coupling parameter for Wild Type glycerol kinase has been found to be approximately 0.08. All of the alanine variants in both domain I and II with the exception of Y39A showed increases in the value of the coupling parameter. However, the increase is significant only for the Q104A variant, as indicated by the uncertainties in the parameter values. W for Y39A variant is equal to 1 since the enzyme was not inhibited even at high concentrations of IIA^{Glc}.

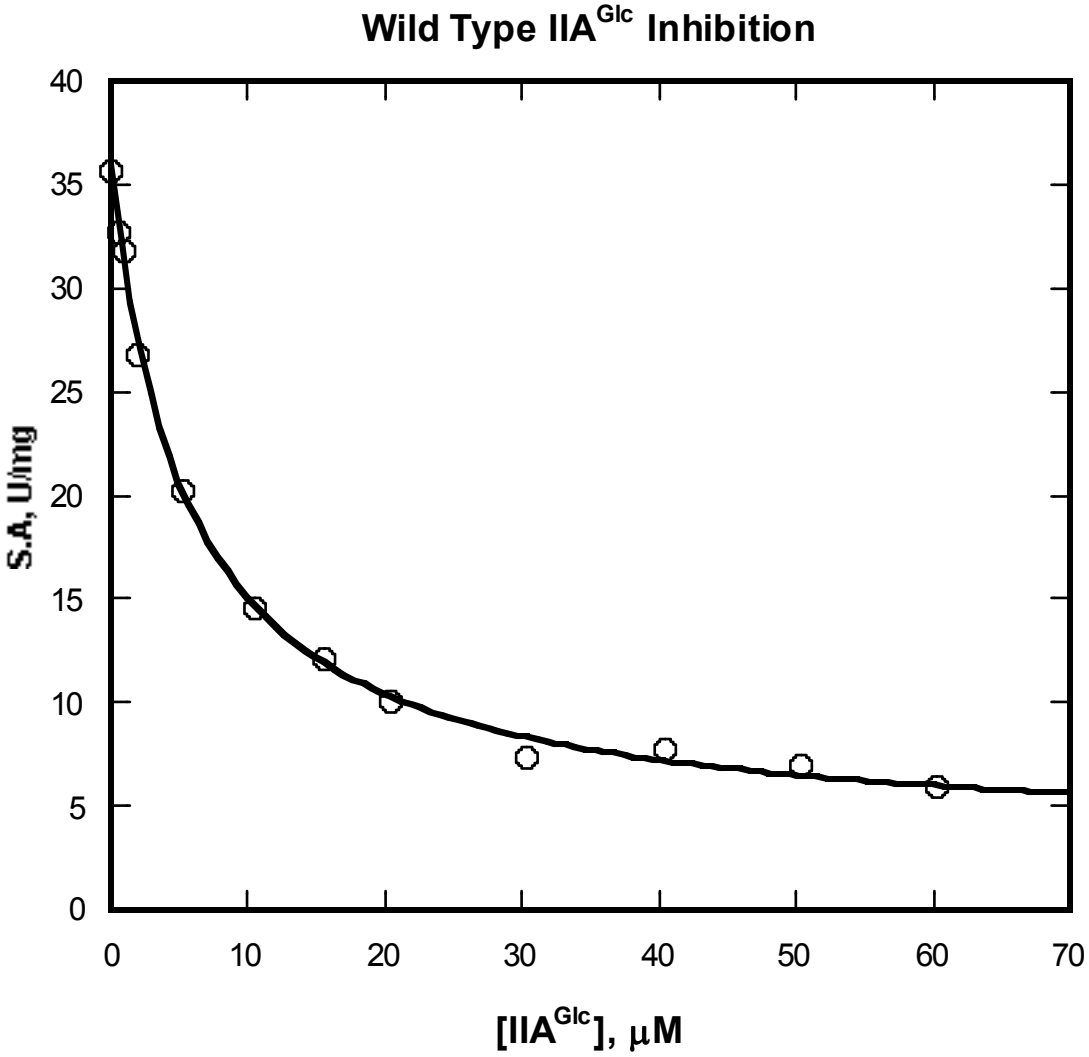

Figure 2: Wild Type IIA^{Glc} inhibition. The curve shows the fit of equation 1 to one of the independent experiments. Each data point is the specific activity determined from the indicated concentrations of IIA^{Glc}. The averaged values of the parameters from the fits of the individual experiments are shown in Table 2. Assay conditions: 2.5 mM ATP, 0.5 μg/mL enzyme.

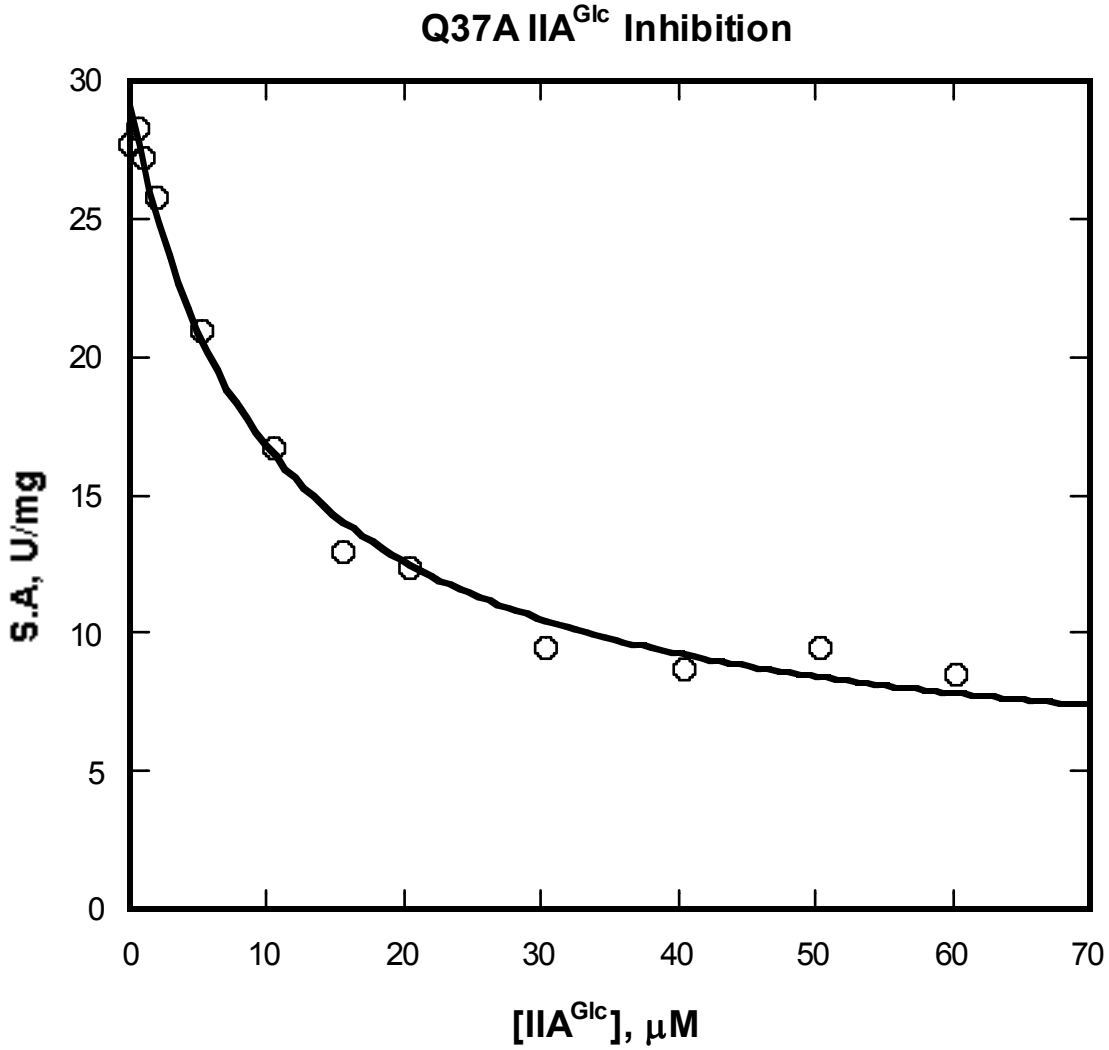

Figure 3: Q37A IIA^{Glc} inhibition. The curve shows the fit of equation 1 to one of the independent experiments. Each data point is the specific activity determined from the indicated concentrations of IIA^{Glc}. The averaged values of the parameters from the fits of the individual experiments are shown in Table 2. Assay conditions: 2.5 mM ATP, 0.5 μg/mL enzyme.

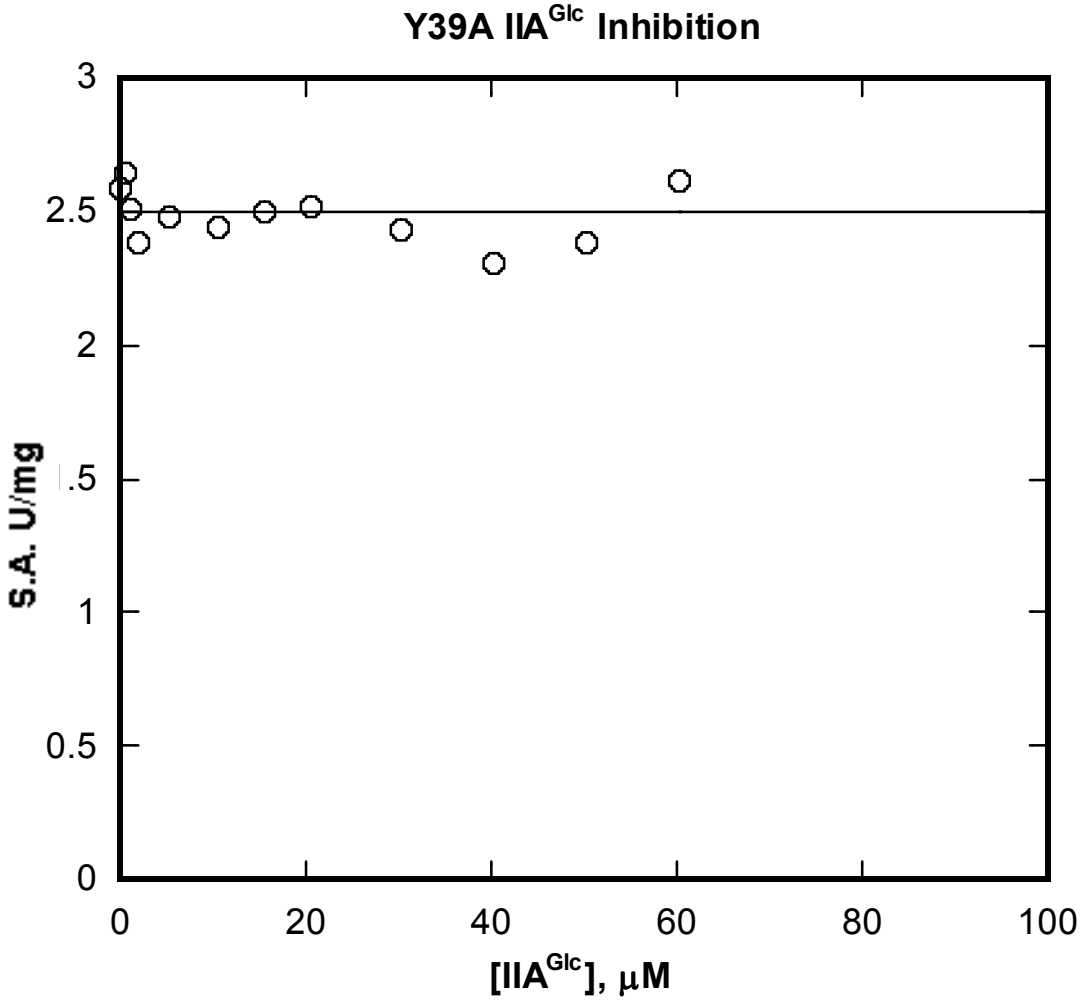

Figure 4: Y39A IIA^{Glc} inhibition. The curve shows the fit of equation 1 to one of the independent experiments. Each data point is the specific activity determined from the indicated concentrations of IIA^{Glc}. The averaged values of the parameters from the fits of the individual experiments are shown in Table 2. Assay conditions: 2.5 mM ATP, 5 μg/mL enzyme.

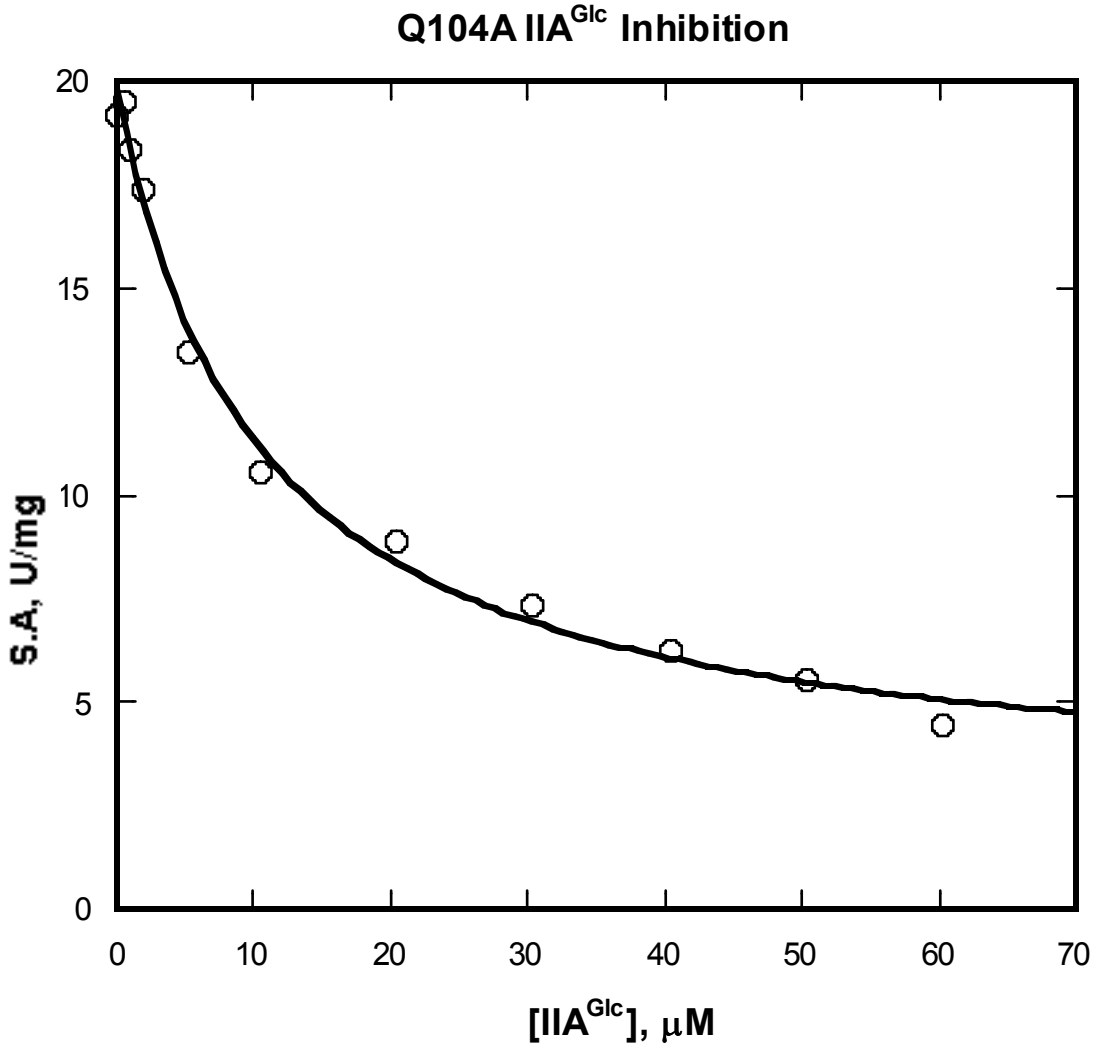

Figure 5: Q104A IIA^{Glc} inhibition. The curve shows the fit of equation 1 to one of the independent experiments. Each data point is the specific activity determined from the indicated concentrations of IIA^{Glc}. The averaged values of the parameters from the fits of the individual experiments are shown in Table 2. Assay conditions: 2.5 mM ATP, 0.1 μg/mL enzyme.

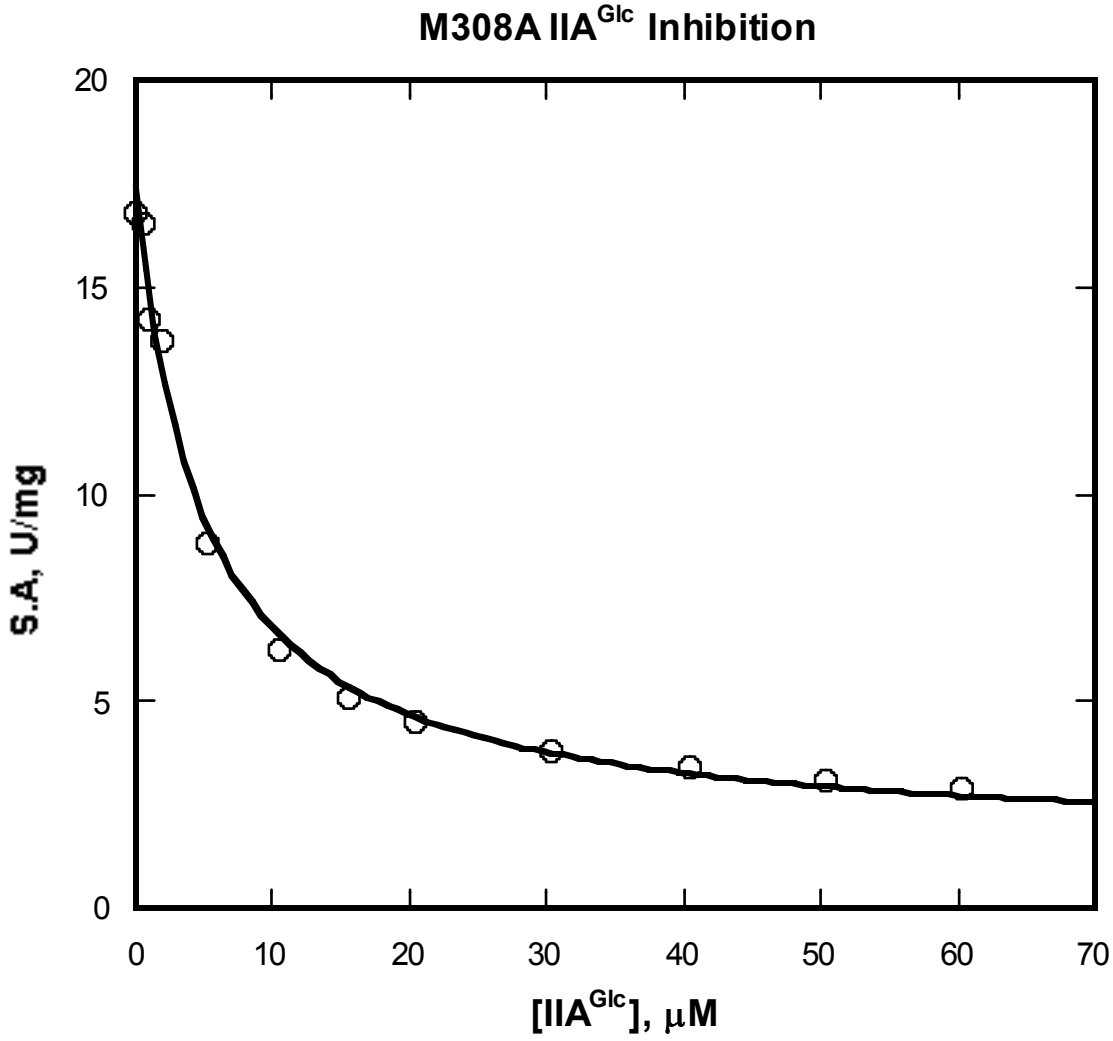

Figure 6: M308A IIA^{Glc} inhibition. The curve shows the fit of equation 1 to one of the independent experiments. Each data point is the specific activity determined from the indicated concentrations of IIA^{Glc}. The averaged values of the parameters from the fits of the individual experiments are shown in Table 2. Assay conditions: 2.5 mM ATP, 5 μg/mL enzyme.

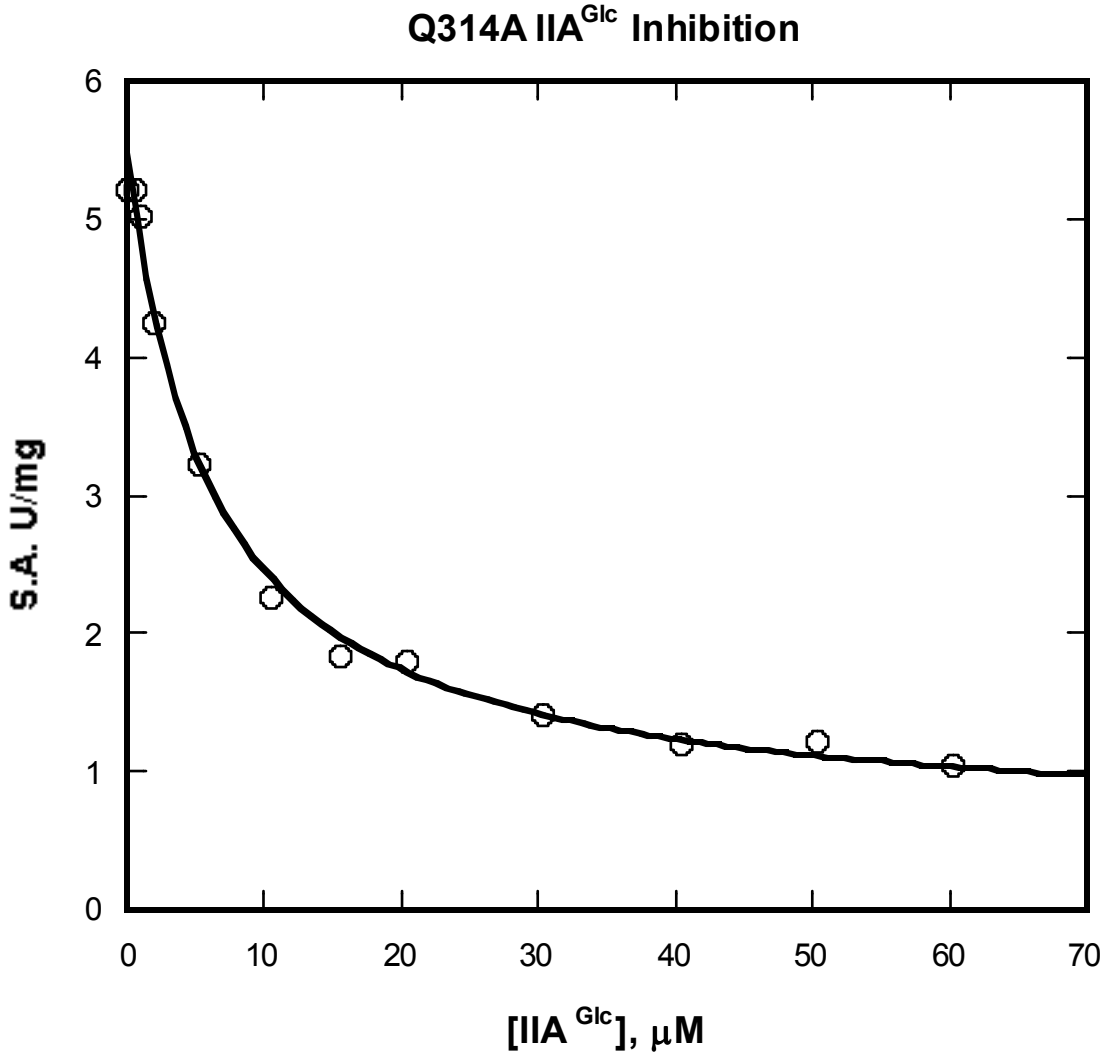

Figure 7: Q314A IIA^{Glc} inhibition. The curve shows the fit of equation 1 to one of the independent experiments. Each data point is the specific activity determined from the indicated concentrations of IIA^{Glc}. The averaged values of the parameters from the fits of the individual experiments are shown in Table 2. Assay conditions: 2.5 mM ATP, 0.5 μg/mL enzyme.

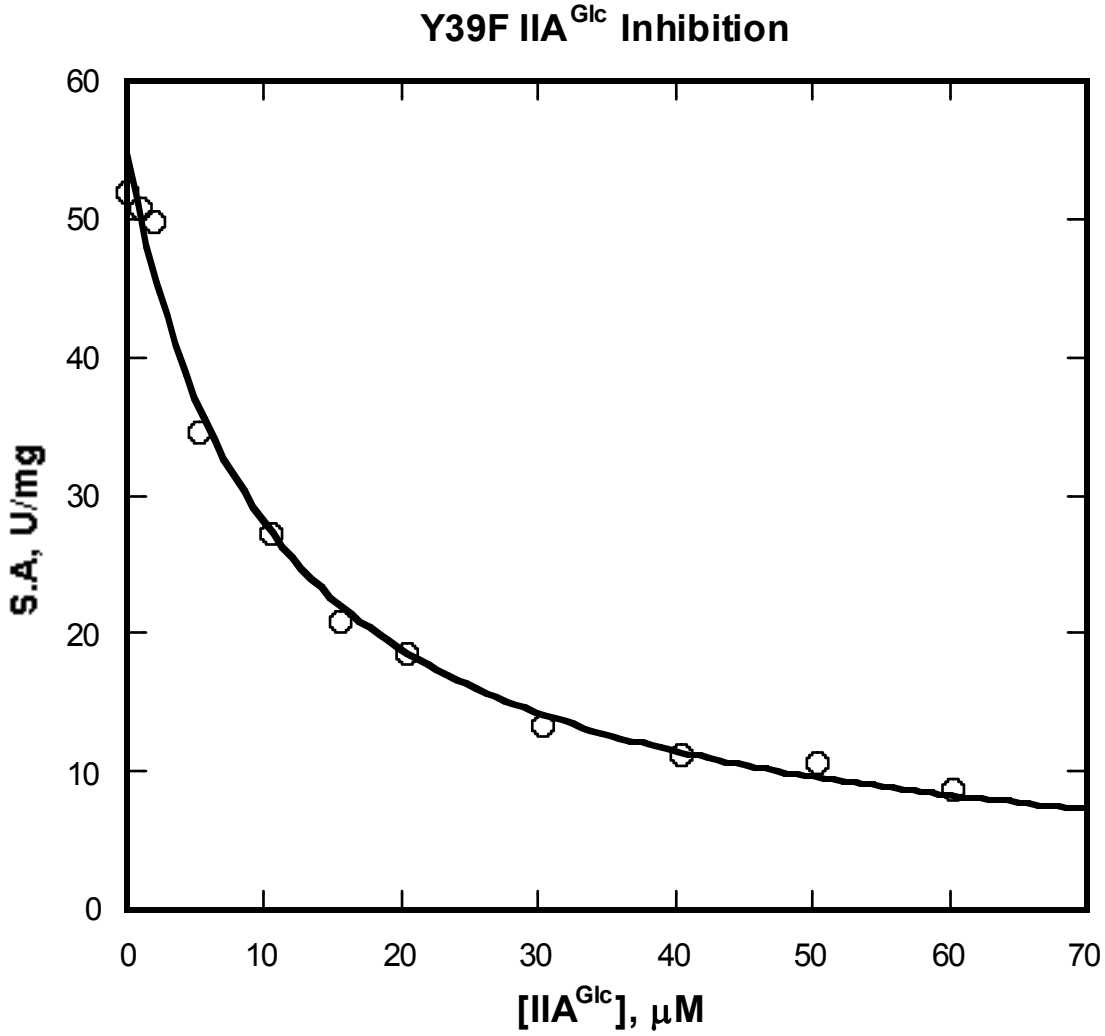

Figure 8: Y39F IIA^{Glc} inhibition. The curve shows the fit of equation 1 to one of the independent experiments. Each data point is the specific activity determined from the indicated concentrations of IIA^{Glc}. The averaged values of the parameters from the fits of the individual experiments are shown in Table 2. Assay conditions: 2.5 mM ATP, 0.5 μg/mL enzyme.

Table 3: IIA^{Glc} inhibition parameters for Wild Type and variant *E. coli* glycerol kinases

	$K_{0.5}$, μM	W
Wild Type	4.6 ± 2.3 (2)	0.08 ± 0.07 (2)
Q37A	9.7 ± 2 (2)	0.13 ± 0.06 (2)
Y39A[a]	ND	1 (4)
Y39F	8.9 ± 1.4 (3)	0.05 ± 0.03 (3)
Q104A	6.8 ± 2.2 (5)	0.22 ± 0.05 (5)
M308A	5.2 ± 0.40 (3)	0.13 ± 0.05 (3)
Q314A[a]	6.2 ± 1.6 (3)	0.12 ± 0.03 (3)

a: These determinations were performed in part by Damien Terry.

Nonlinear least-squares fitting of inhibition data to equation 1 was performed using the computer program Kaleidagraph by Synergy Software to obtain the inhibition parameters $K_{0.5}$. W was determined from equation 2. Numbers in parenthesis indicate the number of independent determinations. The uncertainties shown for the inhibition parameters were determined from the propagated values of the standard errors of parameters obtained where n =2 and from the sample standard deviation where n>2.

ND: Not determined. The $K_{0.5}$ could not be determined because the Y39A enzyme was not found to be inhibited by IIA^{Glc}.

IIA^{Glc} Binding Studies to the Variant Y39A

The apparent loss of IIA^{Glc} inhibition for the Y39A variant raised the question of whether the alanine substitution of Y39 abolished binding or the allosteric coupling to the catalytic site. To address this question of IIA^{Glc} binding to the Y39A variant, a sedimentation velocity method was employed that was previously used to show that the IIA^{Glc} binding site amino acids are not sufficient for transplanting allosteric control into glycerol kinase of another bacterium, *Haemophilus influenzae* (37). This method determines the increase of the sedimentation coefficient for glycerol kinase upon binding to IIA^{Glc}. It benefits from the very low absorbance of IIA^{Glc} at 280 nm due to its lack of tyrosine and tryptophan residues. The sedimentation coefficients were determined as described under Materials and Methods; preliminary results are shown in Table 4. The apparent dissociation constant for the IIA^{Glc} binding to the Y39A variant was determined from the IIA^{Glc} concentration dependence of the sedimentation coefficient and results of those experiments are shown in the figure on page 41. Three different glycerol kinase enzymes were used for those studies: the Wild Type enzyme, the Y39A variant, and an E478C DVN variant. The E478C DVN variant does not bind to IIA^{Glc} because of a steric clash with the aspartate residue at residue 427 (D of DVN). This enzyme serves to measure the effect of solution viscosity increases due to increasing IIA^{Glc} concentrations. The results show a small linear decrease in the sedimentation coefficient for the E478C DVN variant as IIA^{Glc} concentration was increased. This expected small effect was used to correct the apparent sedimentation coefficients for the other two enzymes.

The line through the data points shows the fit to equation 6 to estimate the dissociation constant for IIA^{Glc} binding to EcGK. The sedimentation coefficient of the Wild Type enzyme showed an apparently hyperbolic dependence upon increasing IIA^{Glc} concentration as expected for binding of 4 moles of an 18.1 kDa protein to 1 mole of a 224 kDa protein. In the absence of IIA^{Glc}, the sedimentation coefficient was about 11.1 S, which agrees well with a value of 11.5 S calculated from the tetramer structure using the program HYDROPRO (38). The data are well described by the fitted line, indicating they are consistent with hyperbolic binding of IIA^{Glc} to EcGK. The apparent dissociation constant for the binding was found to be 17 ± 7 μM. This value agrees well with the value of 7 ± 3 μM that is estimated from linked-functions analysis of IIA^{Glc} inhibition (39).

The sedimentation coefficient for the Y39A variant in the absence of IIA^{Glc} was about 10.3, about 1 S less than for Wild Type, indicating that the dimer-tetramer equilibrium is shifted toward the dimer by the substitution. This shift is consistent with reduced apparent affinity for FBP that is described (Table 4).

The sedimentation coefficient for the Y39A variant shows an apparently hyperbolic dependence on IIA^{Glc} concentration, as was seen for the Wild Type enzyme. The data are well described by the fit to equation 5, shown by the line in Figure 9. This result suggests that IIA^{Glc} binding does not affect the dimer-tetramer equilibrium.

The 1 S increase of the sedimentation coefficient for Y39A on addition of IIA^{Glc} was similar to Wild Type, indicating that the Y39A variant binds to IIA^{Glc}.

The apparent dissociation constant for IIA^{Glc} binding to the Y39A variant was found to be 20 ± 6 μM, which agrees well with the dissociation constant obtained for IIA^{Glc} binding to the Wild Type enzyme. This result indicates that the Y39A substitution does not alter the affinity for IIA^{Glc} binding, but completely uncouples the binding from inhibition of catalysis.

Table 4: Sedimentation coefficient parameters for EcGK and Y39A GK variant

	Wild Type EcGK	Y39A EcGK
$S_{20,w}$ (-IIA^{Glc})	11.2	10.3
$S_{20,w}$ (+IIA^{Glc})	12.3	11.1

$S_{20,w}$ – Sedimentation coefficient corrected to 20°C. Concentration of IIA^{Glc} used was 90μM.

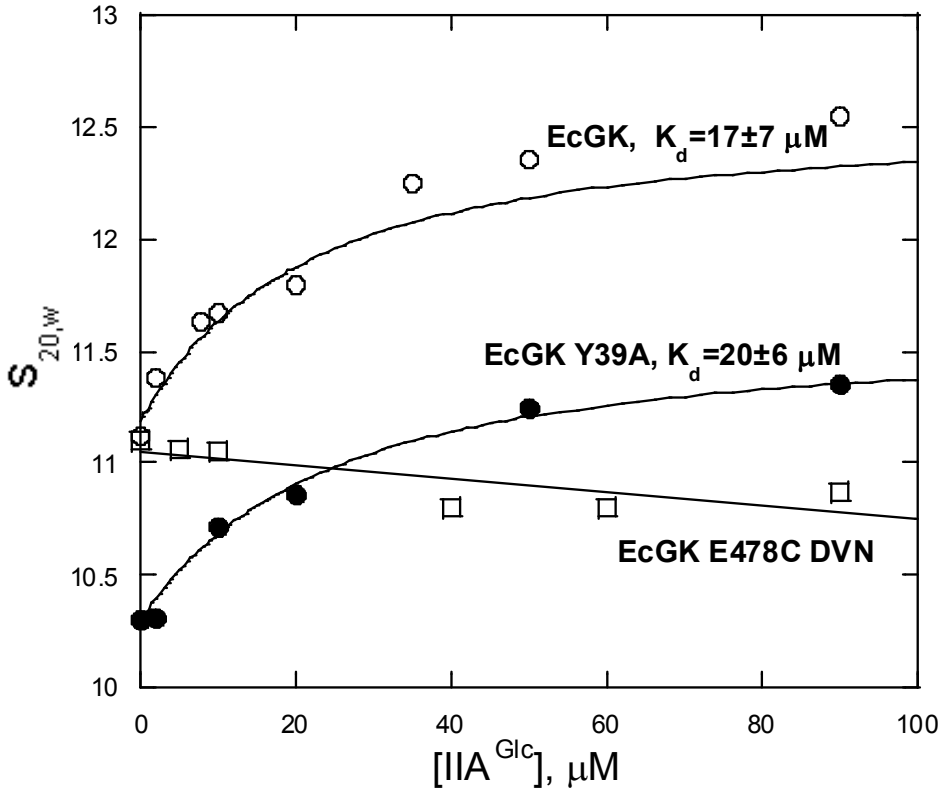

Figure 9: Sedimentation velocity analysis of IIA^{Glc} binding. The lines show the fit of the data for EcGK, Y39A and E478C DVN to equation 6 to give the dissociation constants shown in the figure. The points show the experimentally-determined sedimentation coefficients at the indicated concentration of IIA^{Glc}. The apparent sedimentation coefficients for Wild Type and Y39A glycerol kinase were corrected for viscosity increases using the E478C DVN mutant as a control which does not bind to IIA^{Glc}. Enzyme concentration used was 0.3 mg/ml.

FBP Regulation of Wild Type and Glycerol Kinase Variants

Inhibition by FBP was investigated by assessing the dependence of the activity of the glycerol kinases on FBP concentration as shown in Figures 10-16. FBP concentration was varied from 0 - 10mM and the inhibition parameters of the glycerol kinase variants to FBP determined. The kinetic parameters from the FBP inhibition studies are shown in Table 5. The inhibition parameters $K_{0.5}$ and n_H were determined from fitting the data from the inhibition curves to equation 3 while W was determined from equation 2.

For the domain I variants Q37A, Y39A and Y39F, the $K_{0.5}$ was increased compared to Wild Type. The $K_{0.5}$ of the domain I variant Q104A was not significantly affected by the alanine substitution. For the domain II variants, the affinity of the M308A variant for FBP was increased due to the substitution, showing a two-fold decrease in the $K_{0.5}$ compared to Wild Type glycerol kinase. The $K_{0.5}$ of Q314A was however not affected.

Only two of the variant enzymes, Q37 and Q314 showed changes in W. W was increased slightly by the alanine substitutions of these residues. For all of the variants, FBP inhibition was positively cooperative as for Wild Type glycerol kinase. The Hill coefficient was increased for the Q37A and Q104A variants but was similar to Wild Type for the rest of the mutants. The phenotypes of the variants on MGSA (Table 6) were characteristic of the effects of the substitutions on the $K_{0.5}$; the significance of which are discussed later.

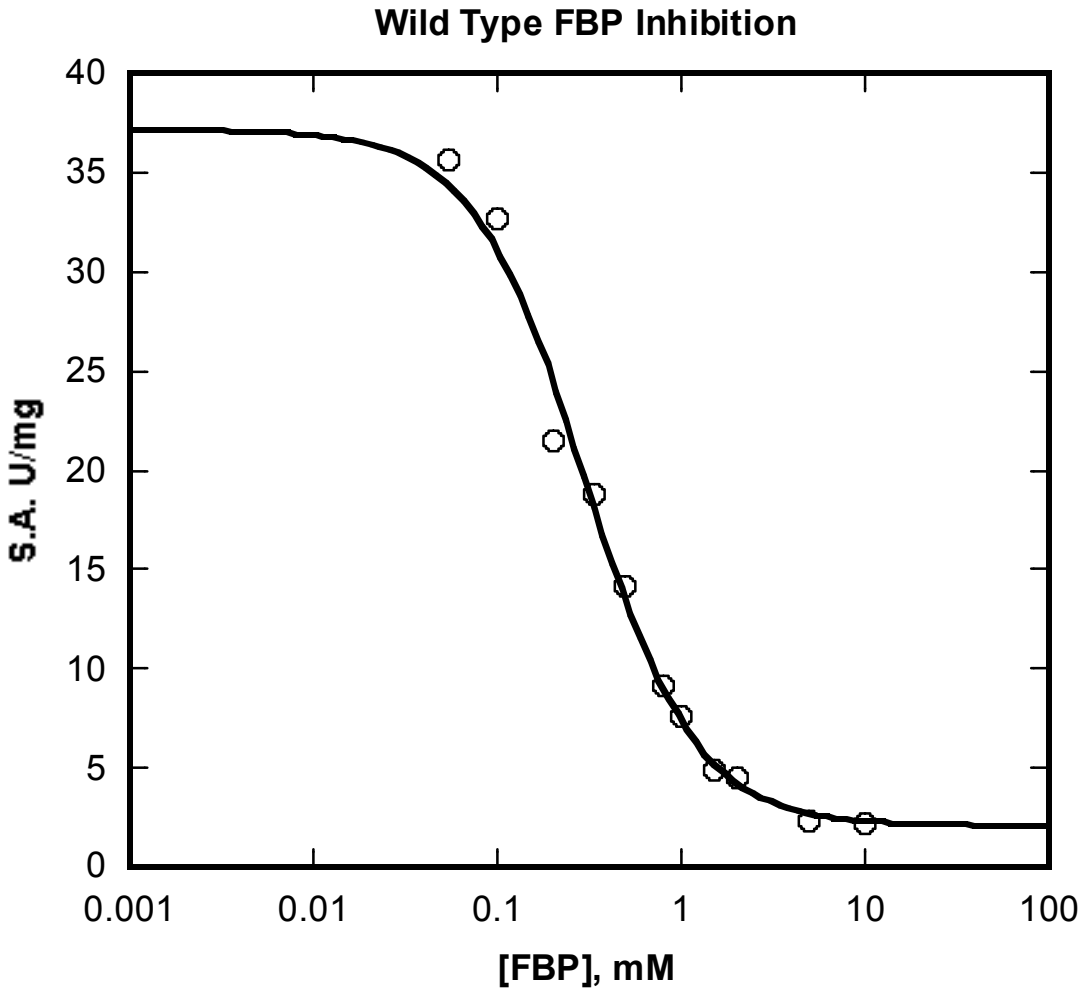

Figure 10: Wild Type FBP inhibition. Each data point is the specific activity determined from the indicated concentrations of FBP. The curve shows the fit of equation 3 to one of the independent experiments. The averaged values of the parameters from the fits of the individual experiments are shown in Table 4. Assay conditions: 2.5 mM ATP, 0.5 μg/mL enzyme.

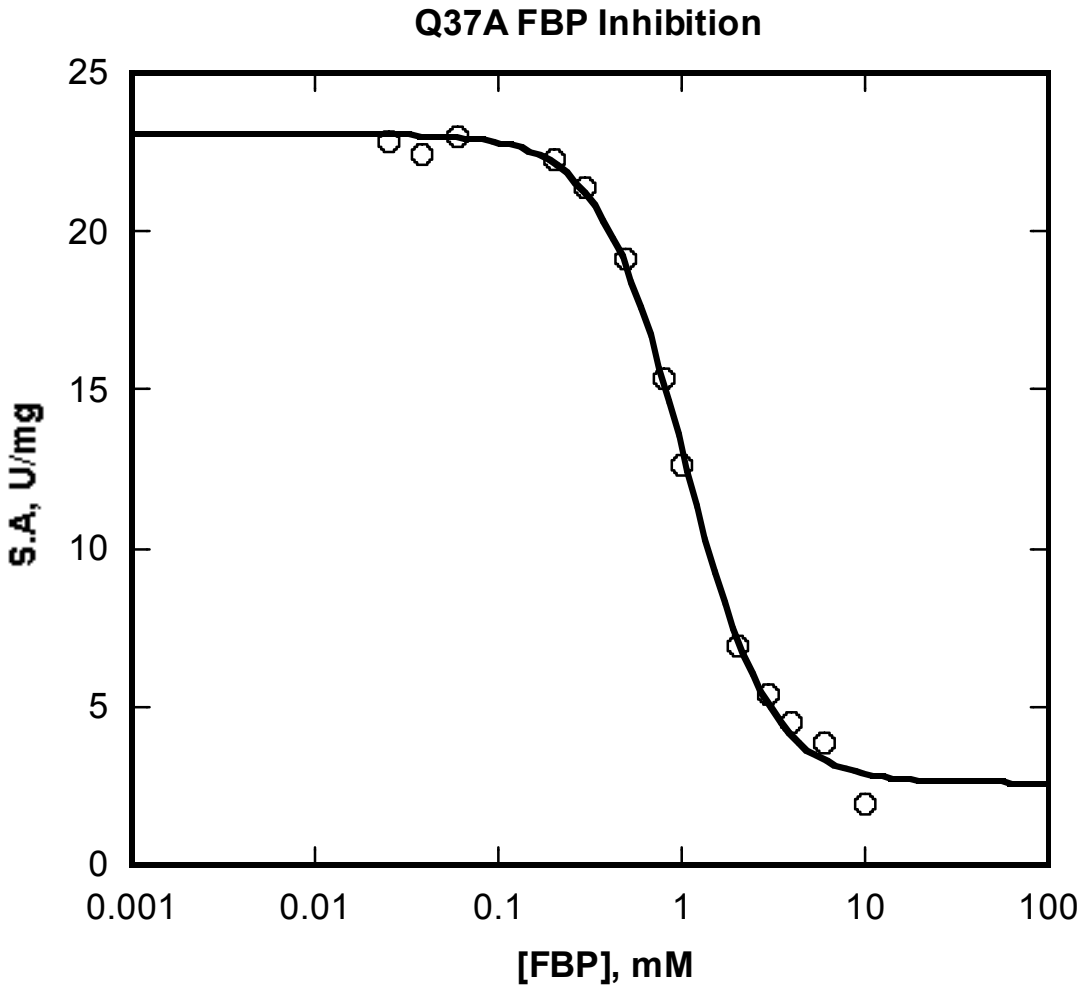

Figure 11: Q37A FBP inhibition. Each data point is the specific activity determined from the indicated concentrations of FBP. The curve shows the fit of equation 3 to one of the independent experiments. The averaged values of the parameters from the fits of the individual experiments are shown in Table 4. Assay conditions: 2.5 mM ATP, 0.5 μg/mL enzyme.

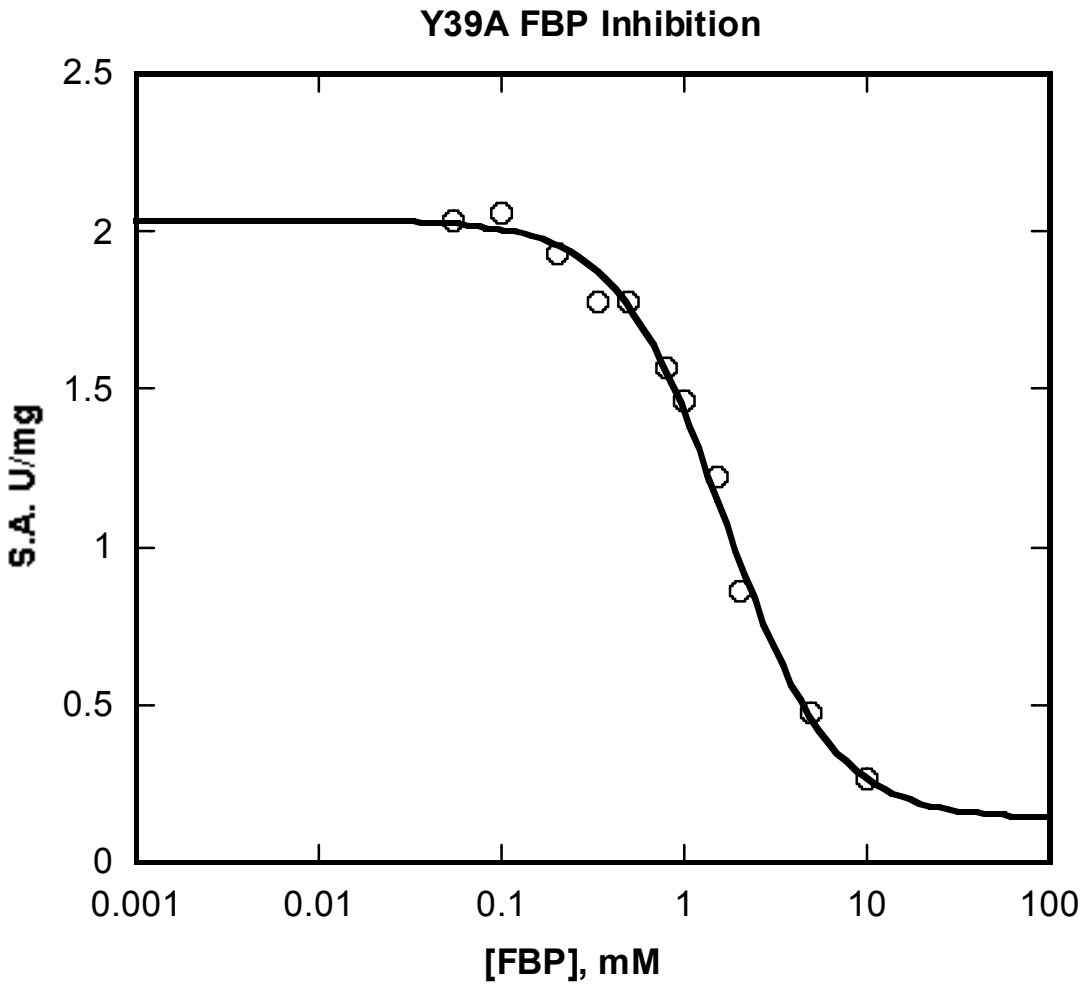

Figure 12: Y39A FBP inhibition. Each data point is the specific activity determined from the indicated concentrations of FBP. The curve shows the fit of equation 3 to one of the independent experiments. The averaged values of the parameters from the fits of the individual experiments are shown in Table 4. Assay conditions: 2.5 mM ATP, 5 μg/mL enzyme.

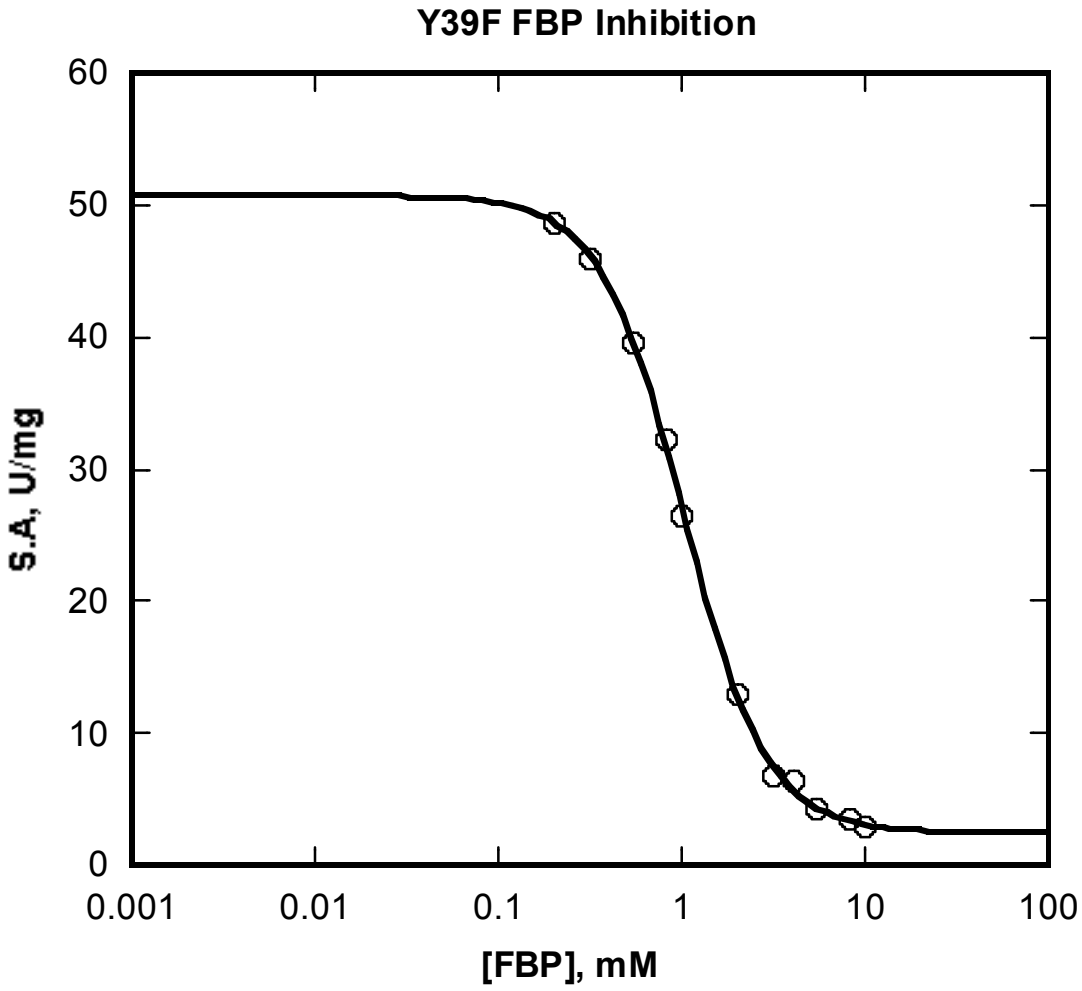

Figure 13: Y39F FBP inhibition. Each data point is the specific activity determined from the indicated concentrations of FBP. The curve shows the fit of equation 3 to one of the independent experiments. The averaged values of the parameters from the fits of the individual experiments are shown in Table 4. Assay conditions: 2.5 mM ATP, 0.5 μg/mL enzyme.

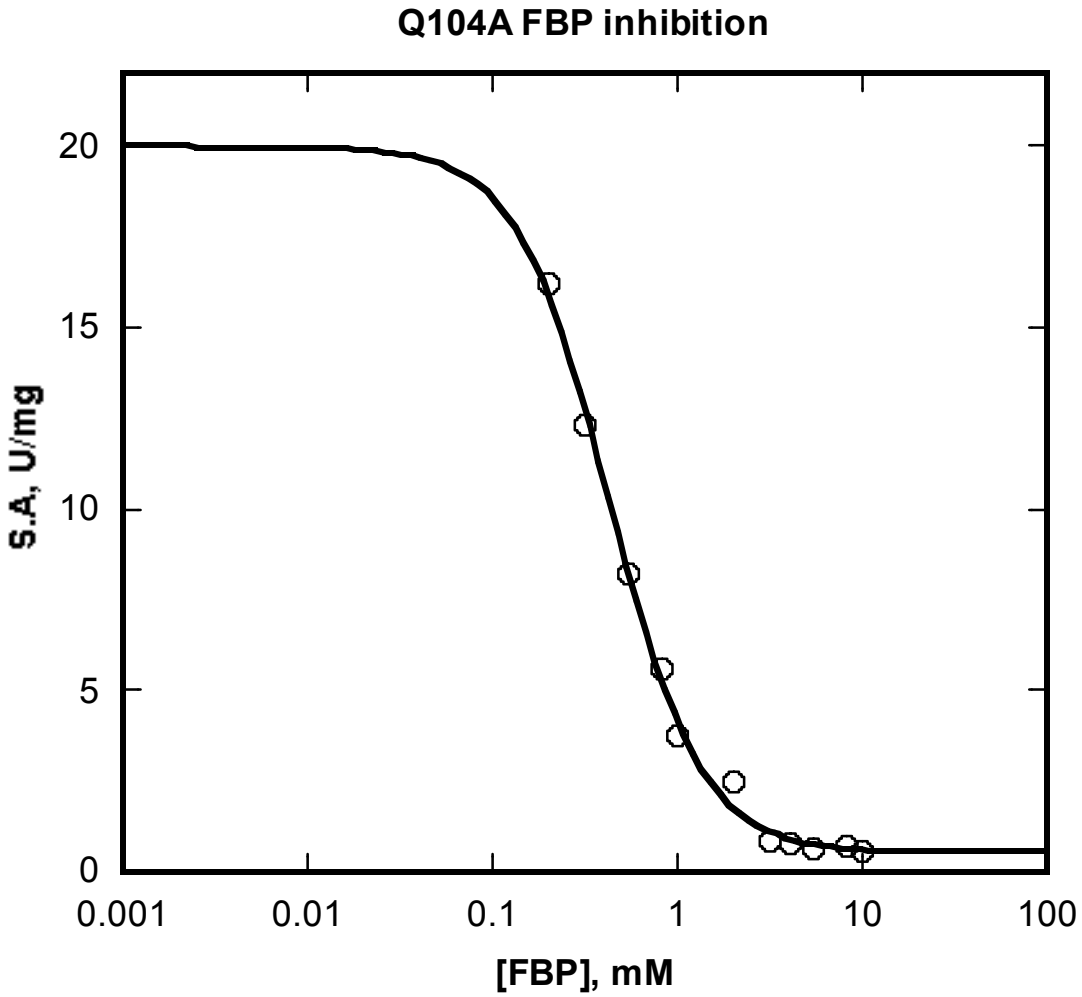

Figure 14: Q104A FBP inhibition. Each data point is the specific activity determined from the indicated concentrations of FBP. The curve shows the fit of equation 3 to one of the independent experiments. The averaged values of the parameters from the fits of the individual experiments are shown in Table 4. Assay conditions: 2.5 mM ATP, 1 μg/mL enzyme.

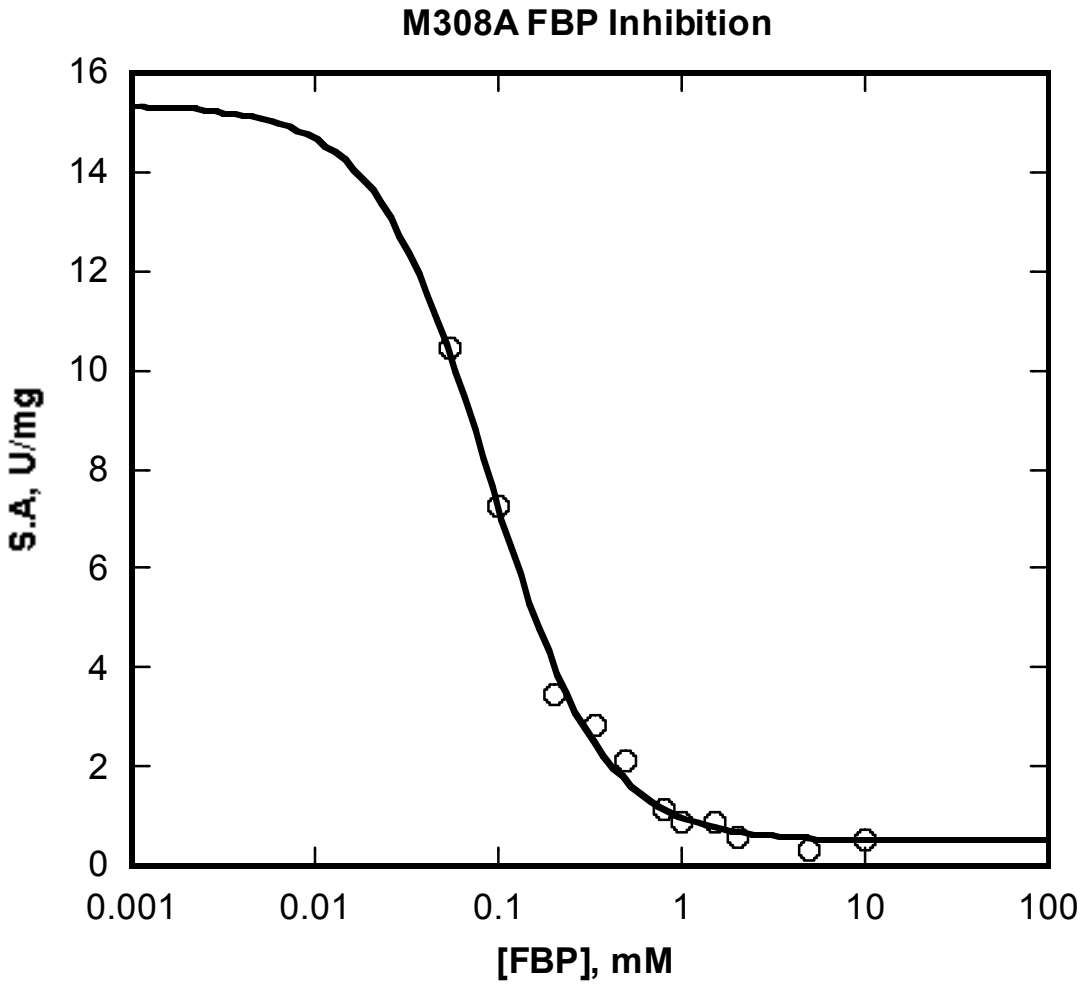

Figure 15: M308A FBP inhibition. Each data point is the specific activity determined from the indicated concentrations of FBP. The curve shows the fit of equation 3 to one of the independent experiments. The averaged values of the parameters from the fits of the individual experiments are shown in Table 4. Assay conditions: 2.5 mM ATP, 5 μg/mL enzyme.

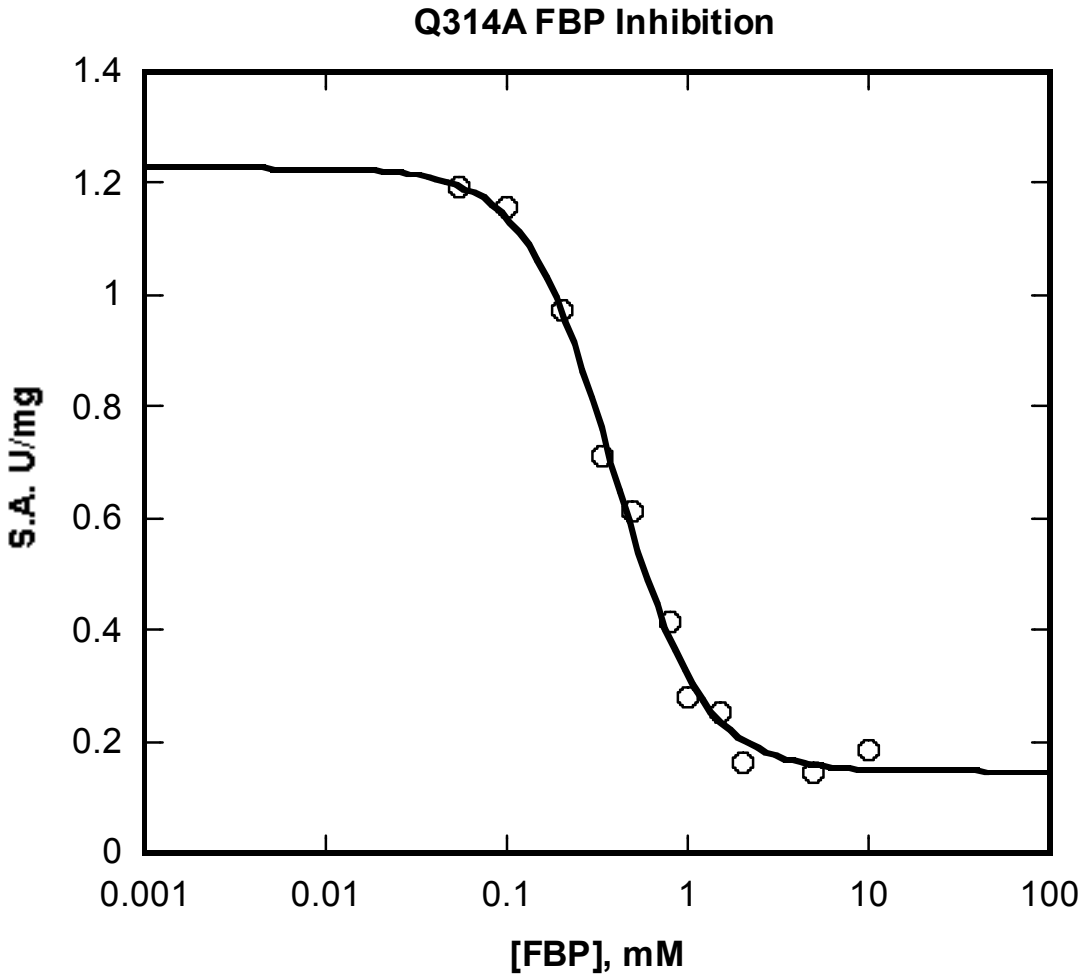

Figure 16: Q314A FBP inhibition. Each data point is the specific activity determined from the indicated concentrations of FBP. The curve shows the fit of equation 3 to one of the independent experiments. The averaged values of the parameters from the fits of the individual experiments are shown in Table 4. Assay conditions: 2.5 mM ATP, 0.5 μg/mL enzyme.

Table 5: FBP inhibition parameters for Wild Type and variant *E. coli* glycerol kinase

	$K_{0.5}$, μM	W	n_H
Wild Type[a]	264 ± 134 (3)	0.04 ± 0.02 (3)	1.2 ± 0.3 (3)
Q37A	1284 ± 247 (3)	0.15 ± 0.09 (3)	1.9 ± 0.8 (3)
Y39A	1722 ± 204 (2)	0.06 ± 0.06 (2)	1.4 ± 0.2 (2)
Y39F	965 ± 74 (3)	0.04 ± 0.01 (3)	2.0 ± 0.1 (3)
Q104A	425 ± 9 (3)	0.02 ± 0.01 (3)	1.7 ± 0.1 (3)
M308A	97 ± 19 (2)	0.04 ± 0.02 (2)	1.5 ± 0.2 (2)
Q314A[a]	317 ± 30 (2)	0.11 ± 0.04 (2)	1.6 ± 0.3 (2)

a: These determinations were performed in part by Damien Terry

Nonlinear least-squares fitting of inhibition data to equation 3 was performed using the computer program Kaleidagraph by Synergy Software to obtain the inhibition parameters $K_{0.5}$ and n_H. W was determined from equation 2. Numbers in parenthesis indicate the number of independent determinations. The uncertainties shown for the inhibition parameters were determined from the propagated values of the standard errors of parameters obtained where n=2 and from the sample standard deviation where n>2.

Table 6: Phenotypes of cells transformed with variant glycerol kinase

E. coli Glycerol Kinase	Phenotype of Colonies on MGSA plates
Wild Type	Purple
Q37A	Purple with foggy halo
Y39A	Purple with foggy halo
Y39F	Purple with slightly foggy halo
Q104A	Purple with slightly foggy halo
M308A	Pink
Q314A	Purple

The phenotypes of the variant *E. coli* were recorded after overnight growth on MGSA plates.

Effects of the Domain Bridging Amino Acid Substitutions on Enzyme Catalytic Properties

Initial velocity kinetic studies for each of the variant glycerol kinases were performed in the forward direction using the ADP coupled spectrophotometric assay at pH 7.0 and 25°C with a Beckman DU800 spectrophotometer. In each of the assays, glycerol was added to the enzyme to a final concentration of 10 mM. The dependence of the initial velocity of Wild Type and each glycerol kinase variant on the concentration of the substrate ATP is shown in Figures 17-23. The kinetic data obtained from the assays were fit to equation 4 in Materials and Methods. The kinetic constants were obtained from the fits of at least two independent experiments and are shown in Table 7.

Considering domain I, the alanine substitutions had the effect of reducing the V_{max} in Q37A and Y39A. The reduction in V_{max} was most pronounced and significant in Y39A. Compared to the V_{max} of the Wild Type enzyme, Q37A was reduced two-fold, while Y39A was reduced four-fold. The V_{max} of Y39F was however unaffected by the substitutions, while it was increased for the Q140A variant. For domain II, the V_{max} of M308A was significantly affected, with a three-fold reduction while the V_{max} of Q314A was slightly increased by the substitution.

The Michaelis constant (K_m) for ATP of Wild Type glycerol kinase was also compared to the variant enzymes. The K_m of the domain I variants Q37A and Y39F were not significantly affected. The alanine substitutions in Y39 and Q104 however resulted in an increased K_m. The K_m of Y39A was increased about twelve-fold higher than that of Wild Type glycerol kinase while Q104A had an approximately seven-fold increase in

the K_m. In the determination of the K_m for Y39A and Q104A, the apparent binding affinity for ATP of these variants appeared to shift the K_m to the right. The ATP concentrations were therefore varied up to 2.5 mM. Considering domain II, the K_m was not affected by the alanine substitution of both M308 and Q314.

Due to the observed large effects of the Y39A substitution on the enzyme catalytic properties as had been observed for IIA^{Glc} inhibition, the second substrate glycerol was varied to obtain the Michaelis constant for glycerol and the dissociation constant for ATP. The results are shown in Table 8. The V_{max} and K_m for ATP for the Y39A variant determined from both substrates agreed well with the value obtained from varying ATP alone. There was a significant increase in the K_m for ATP and a decrease in the V_{max}. The results showed that the K_m for glycerol was also increased about 21-fold higher for Y39A compared to Wild Type. The dissociation constants (K_{ia}) determined showed that the alanine substitution of Y39 resulted in a decrease in the K_{ia} for ATP.

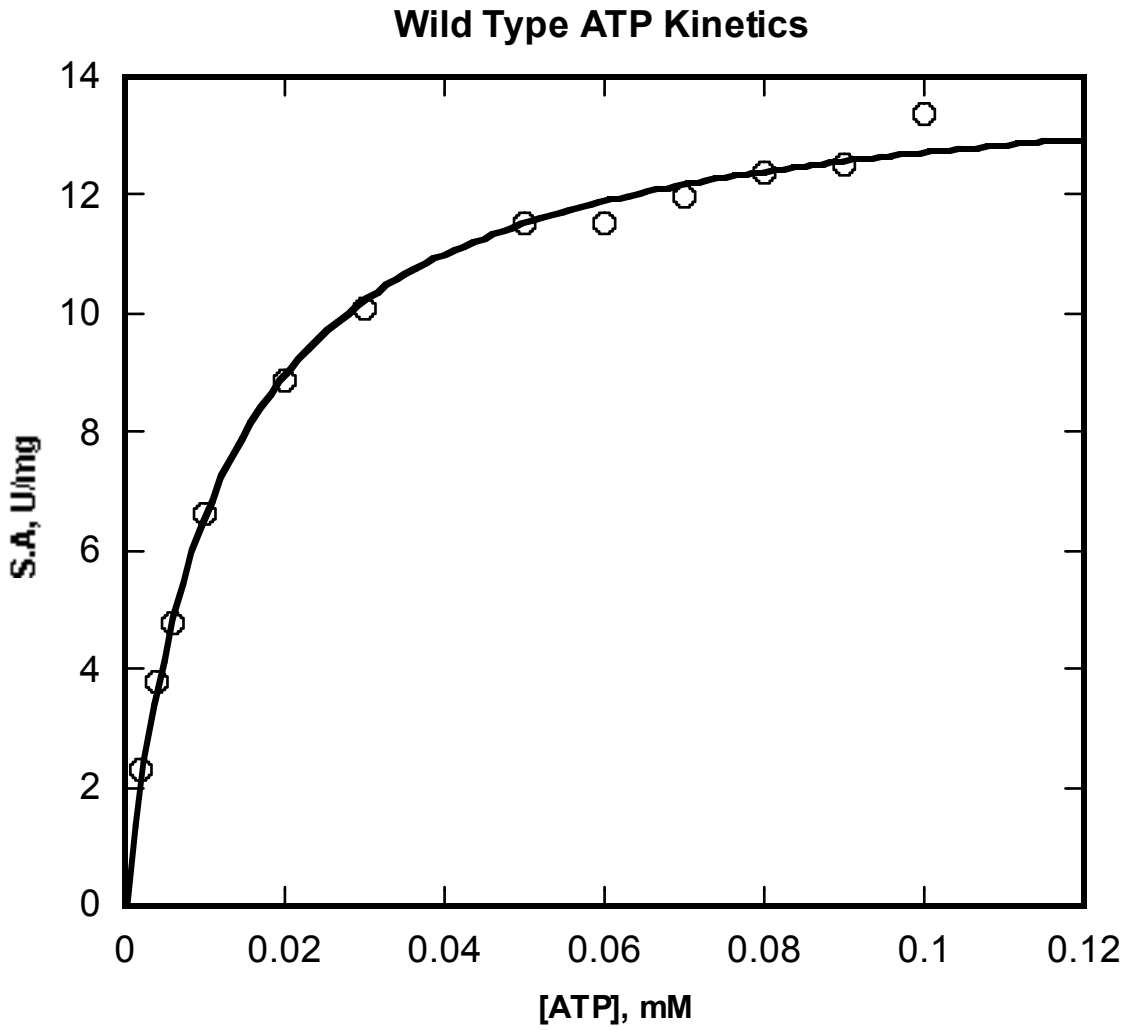

Figure 17: Wild Type ATP kinetics. Each data point is the specific activity determined from the indicated concentrations of ATP. The curve shows the fit to equation 4 to one of the independent experiments. The parameters from the average fit are shown in Table 5. The enzyme concentration used in each assay was 0.5 μg/mL.

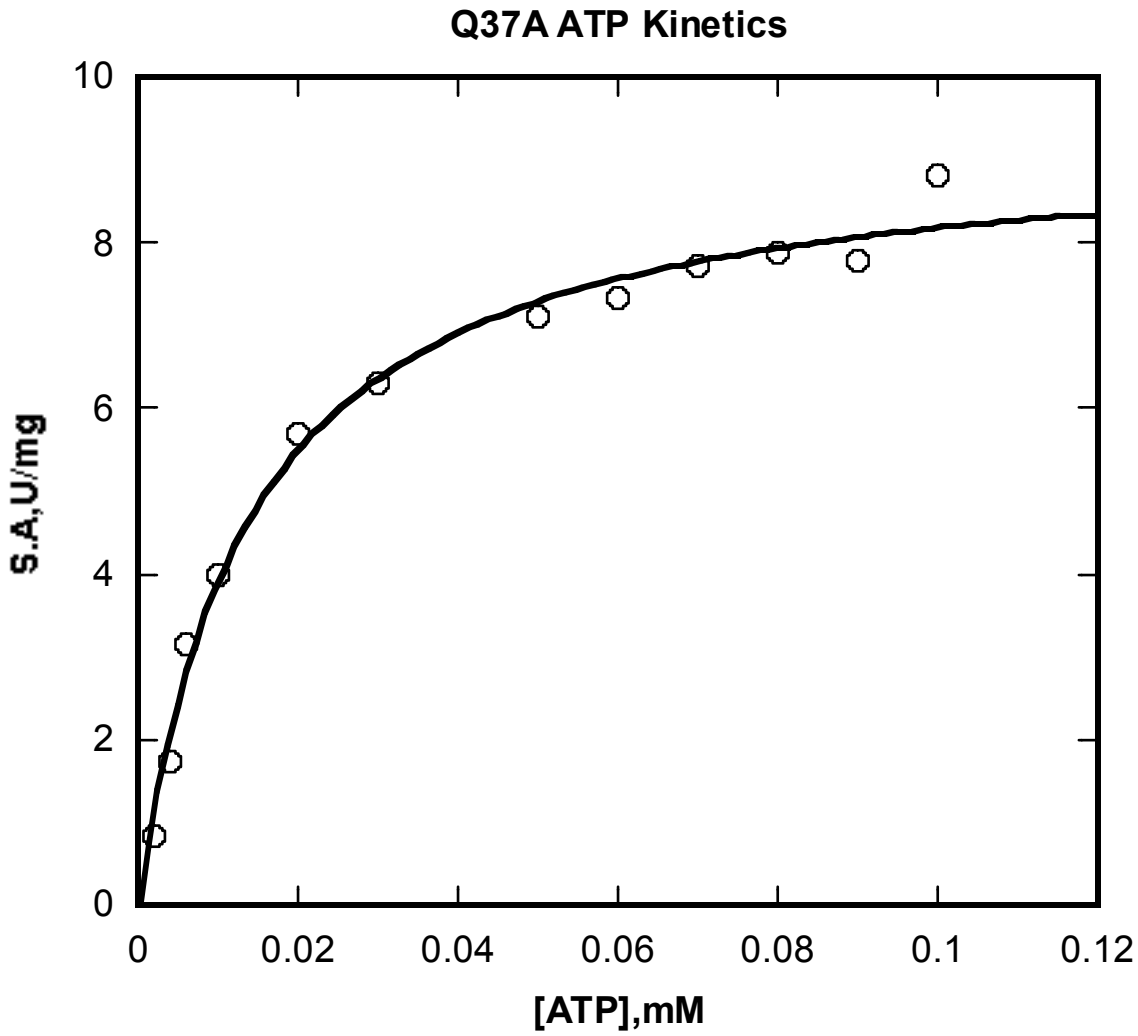

Figure 18: Q37A ATP kinetics. Each data point is the specific activity determined from the indicated concentrations of ATP. The curve shows the fit to equation 4 to one of the independent experiments. The averaged values of the parameters from the fits of the individual experiments are shown in Table 5. The enzyme concentration used in each assay was 0.5 μg/mL.

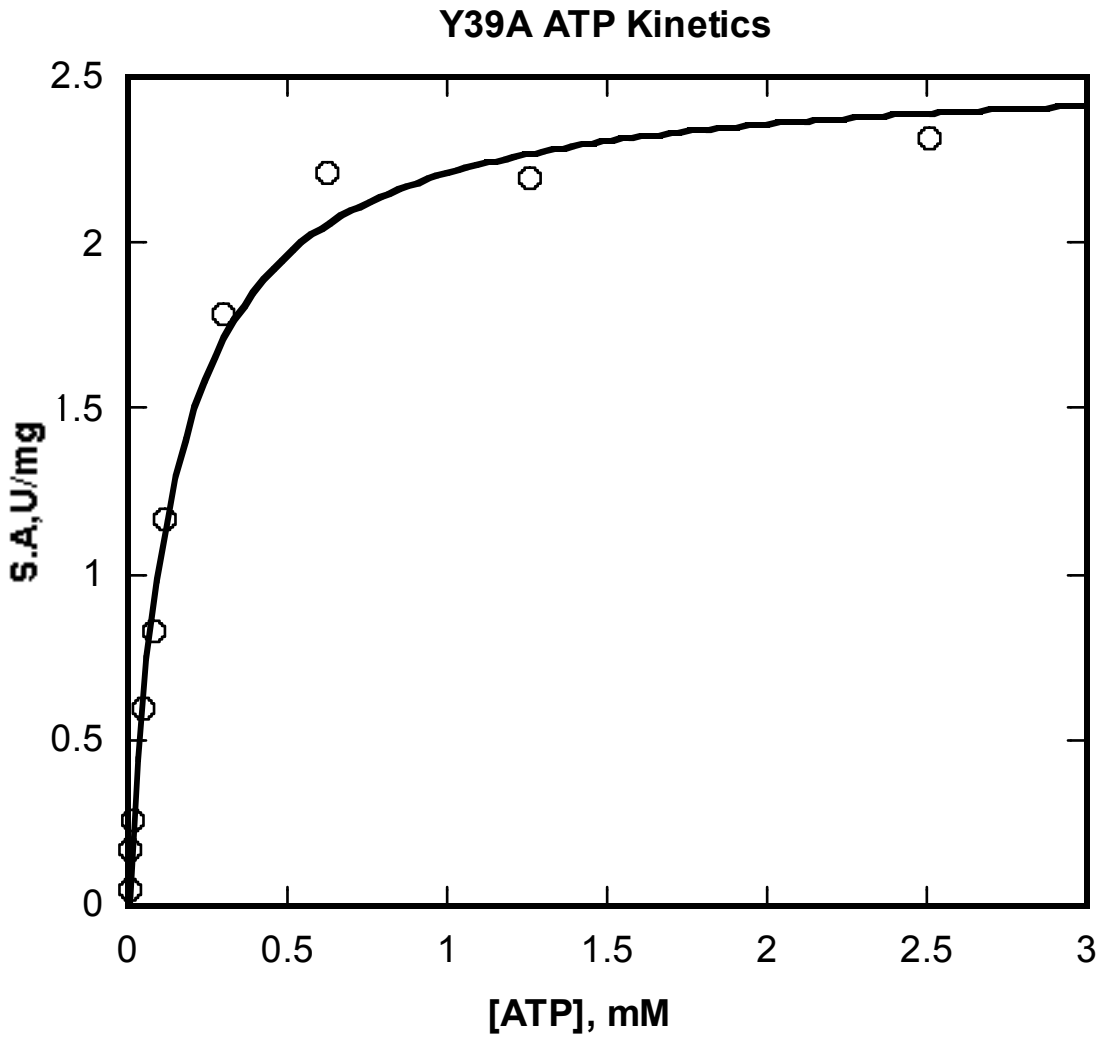

Figure 19: Y39A ATP kinetics. Each data point is the specific activity determined from the indicated concentrations of ATP. The curve shows the fit to equation 4 to one of the independent experiments. The averaged values of the parameters from the fits of the individual experiments are shown in Table 5. The enzyme concentration used in each assay was 5 μg/mL.

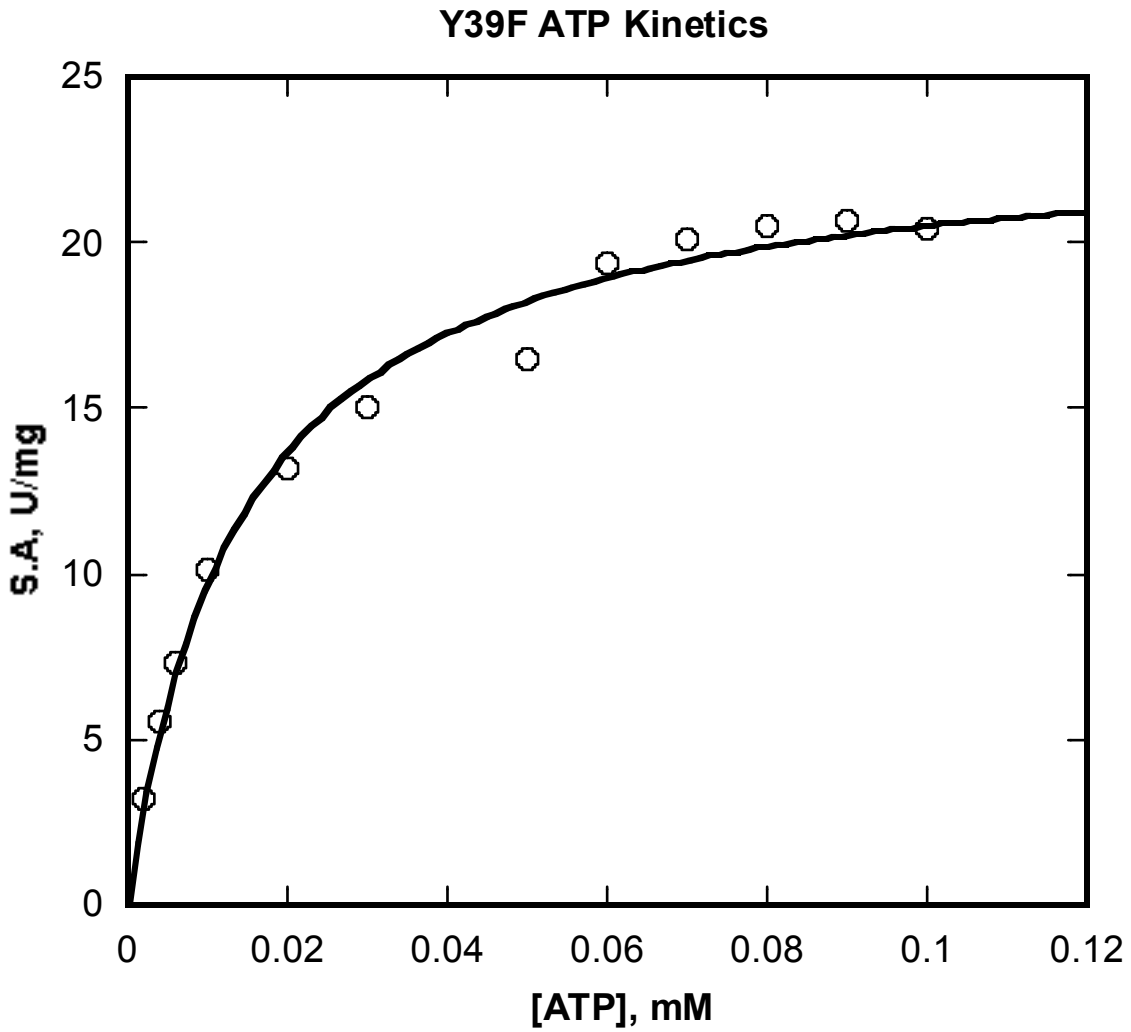

Figure 20: Y39F ATP kinetics. Each data point is the specific activity determined from the indicated concentrations of ATP. The curve shows the fit to equation 4 to one of the independent experiments. The parameters from the average fit are shown in Table 5. The enzyme concentration used in each assay was 0.5 μg/mL.

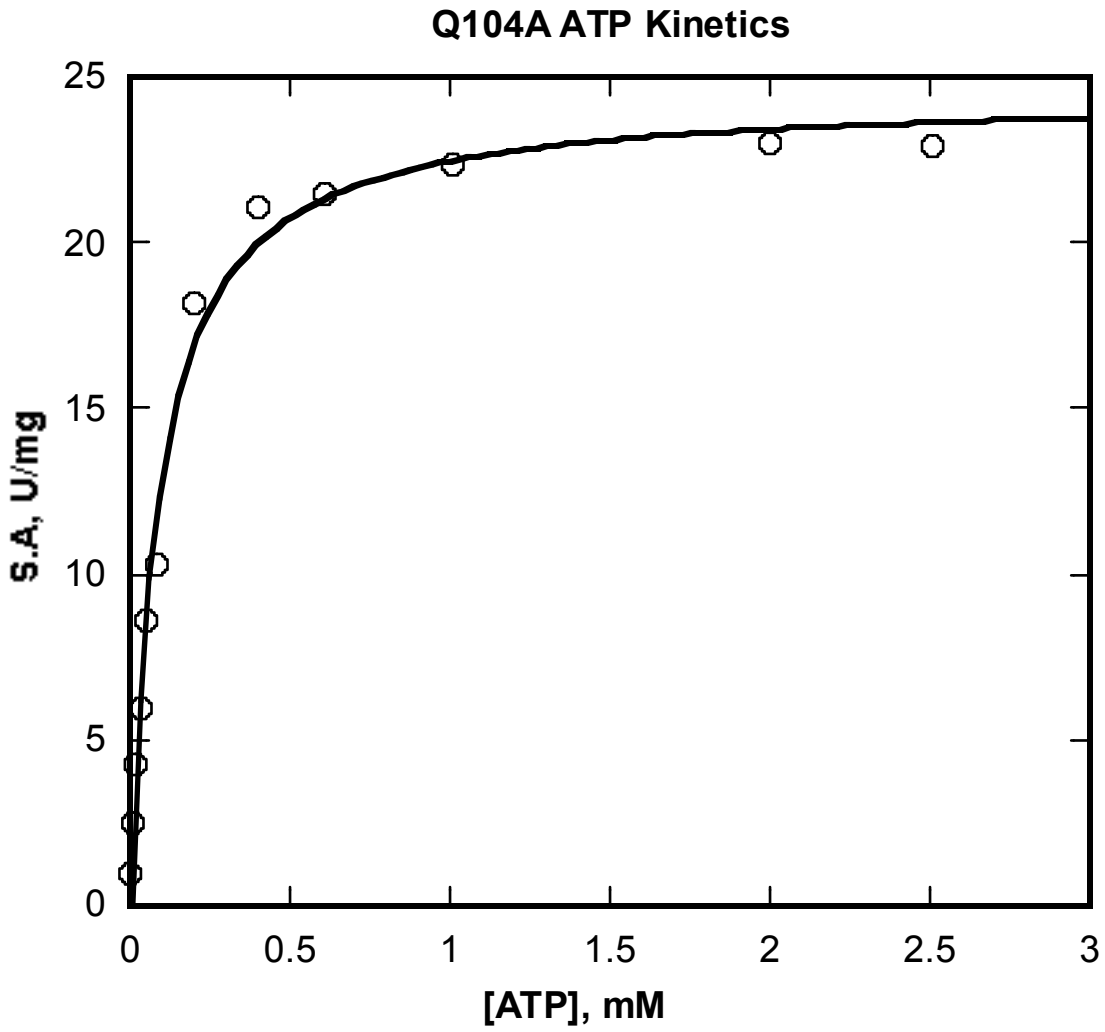

Figure 21: Q104A ATP kinetics. Each data point is the specific activity determined from the indicated concentrations of ATP. The curve shows the fit to equation 4 to one of the independent experiments. The parameters from the average fit are shown in Table 5. The enzyme concentration used in each assay was 1 μg/mL.

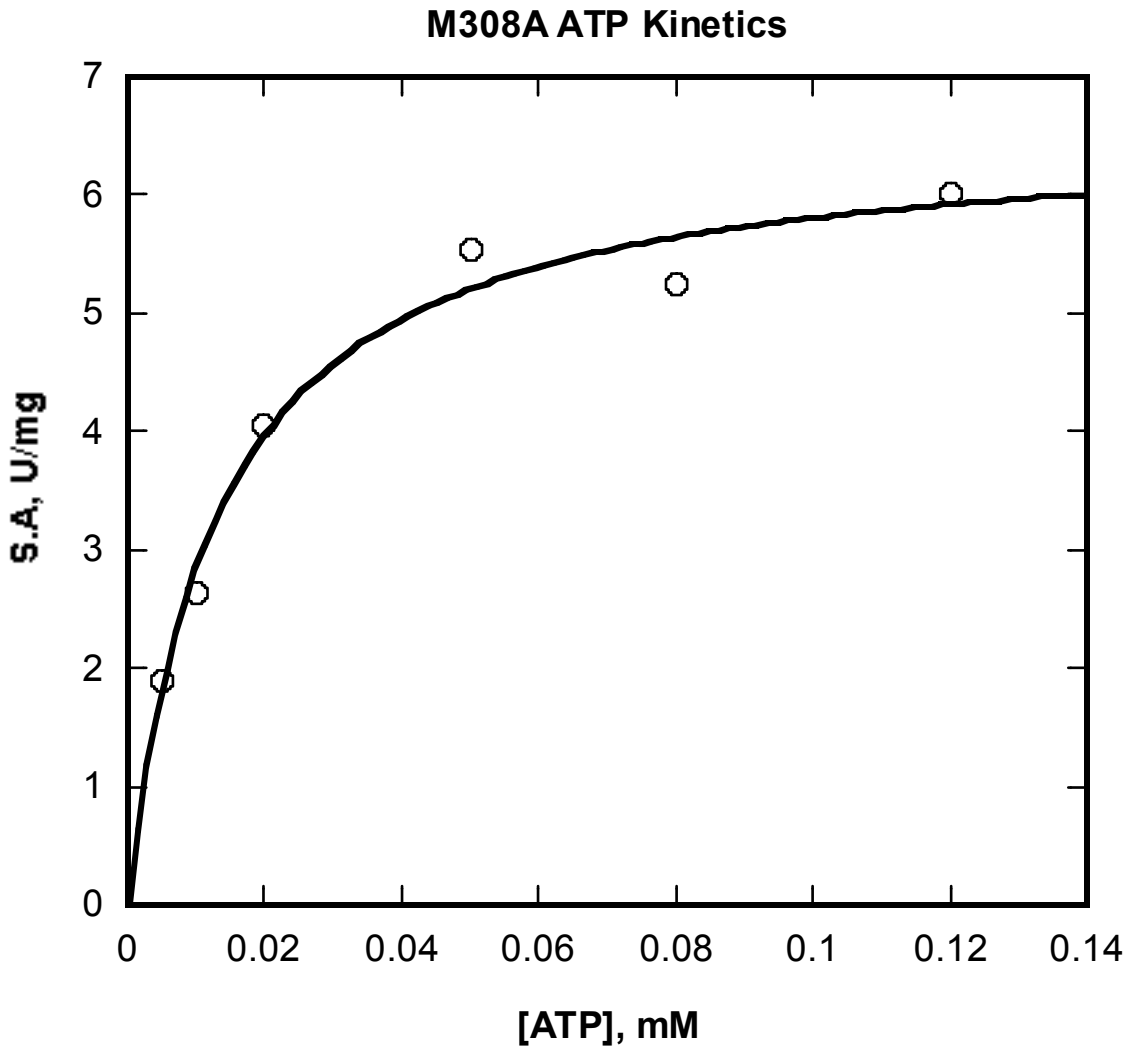

Figure 22: M308A ATP kinetics. Each data point is the specific activity determined from the indicated concentrations of ATP. The curve shows the fit to equation 4 to one of the independent experiments. The parameters from the average fit are shown in Table 5. The enzyme concentration used in each assay was 5 μg/mL.

.

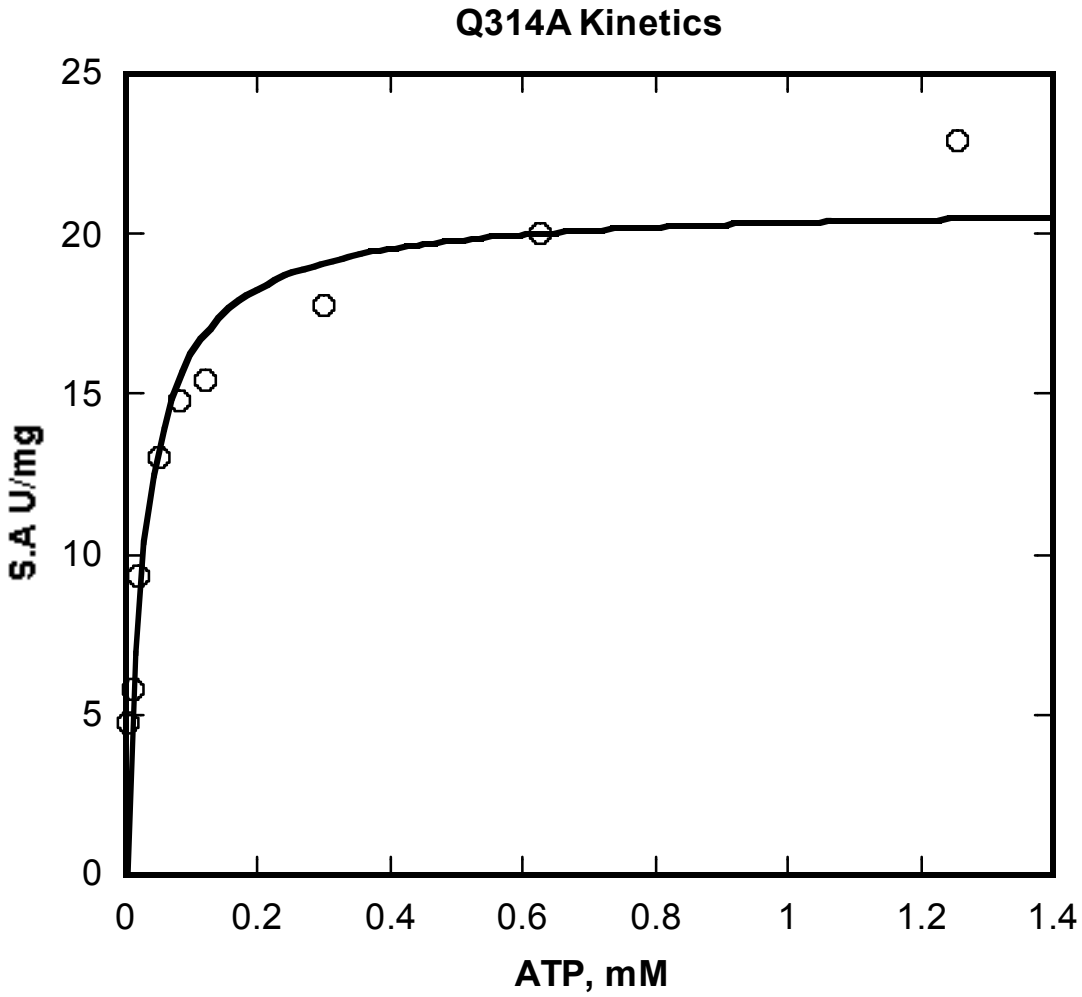

Figure 23: Q314A ATP kinetics. Each data point is the specific activity determined from the indicated concentrations of ATP. The curve shows the fit to equation 4 to one of the independent experiments. The parameters from the average fit are shown in Table 5. The enzyme concentration used in each assay was 0.5 μg/mL.

Table 7: Steady state kinetics for Wild Type and variant *E. coli* glycerol kinase

	V_{max}, U/mg	K_m^{ATP}, μM
Wild Type[a]	12.9 ± 4.6 (2)	11.1 ± 13 (2)
Q37A	8.6 ± 0.7 (2)	15.8 ± 4 (2)
Y39A	3.4 ± 0.2 (2)	136 ± 29 (2)
Y39F	21.4 ± 2.7 (3)	11.7 ± 2.7 (3)
Q104A	22.5 ± 4.3 (3)	78 ± 25 (3)
M308A[a]	6.6 ± 0.3 (1)	12.6 ± 3.4 (3)
Q314A[a]	20.9 ± 0.9 (1)	14.8 ± 2.8 (3)

a: These determinations were performed in part by Damien Terry

Nonlinear least-squares fitting of inhibition data to equation 4 was performed using the computer program Kaleidagraph by Synergy Software to obtain the inhibition parameters V_{max} and K_m^{ATP}. Numbers in parenthesis indicate the number of independent determinations. The uncertainties shown for the inhibition parameters were determined from the propagated values of the standard errors of parameters obtained where n=2 and from the sample standard deviation where n>2. Where n=1, the enzyme was not found to be stable in the crystalline ammonium sulfate form it was stored in, resulting in an irreversible loss of activity which prevented the accurate determination of the V_{max} over time. The reported vaules are therefore for the earliest determination. The uncertainties shown for the single determinations are the standard errors of the parameters.

Table 8: Michaelis and dissociation constants of Wild Type and Y39A glycerol kinase

	V_{max}, U/mg	K_m for ATP, μM	K_{ia} for ATP, μM	K_m for glycerol, μM
Wild Type	15.7 ± 0.3 [a]	11.7 ± 0.7	86 ± 25[a]	4.9 ± 1.2 [a]
Y39A[b]	5.1 ± 0.1	110 ± 8	43 ± 15	105 ± 7

a: Results from Pettigrew et al., (12).
b: These determinations were performed by Shanna Mayorov.

Nonlinear least-squares fitting of inhibition data to equation 5 was performed using the computer program EnzFitter (Biosoft, Cambridge, U.K) to obtain the inhibition parameters $V_{max,}$ K_m for ATP, K_{ia} for ATP, and K_m for glycerol. The uncertainties shown for the inhibition parameters are the standard errors for the parameters.

CHAPTER IV

DISCUSSION

Five amino acids were identified to be within 7 Å of an Arg^{369} residue which was found to be important in IIA^{Glc} inhibition. Three of the amino acids (Q37, Y39 and Q104) bridge domain I and Arg^{369} of EcGK while the other two bridge domain II and Arg^{369} of EcGK. This work used structure perturbation studies to understand the role of these domain bridging interactions in the regulation of EcGK by the allosteric inhibitor IIA^{Glc}. The effects of the substitutions on FBP inhibition and catalytic properties of the enzyme were also assessed.

Importance of the Domain Bridging Amino Acids in IIA^{Glc} Regulation of EcGK

The effects of the substitutions of the domain bridging amino acids on the regulation of the EcGK by the inhibitors IIA^{Glc} are discussed. IIA^{Glc} inhibition for the domain I mutants were interesting since Y39A exhibited no IIA^{Glc} inhibition, while Q37A and Q104A had reduced affinity for IIA^{Glc}. The inhibition parameter, $K_{0.5}$, is the apparent dissociation constant for allosteric effector binding and gives an indication of the binding affinity of the allosteric effector to the enzyme. The increased $K_{0.5}$ values of the domain I alanine variants of Q37 and Q104 therefore suggest that the interactions of the domain I residues are important for regulating binding of the inhibitor IIA^{Glc} to the EcGK enzyme. The interaction of Y39 with Arg^{369} seems particularly important in coupling binding with IIA^{Glc} inhibition. This is because the Y39A substitution had the

effect of causing a lack of inhibition of the EcGK enzyme. The sedimentation velocity experiments however showed that the IIA^{Glc} was still binding to the Y39A variant. The alanine substitution of this residue therefore appeared to uncouple binding of IIA^{Glc} and inhibition. The coupling factor, W, was increased for the domain I residues Q37, Y39 and Q104. The increase was however only significant for the Y39A variant. The value of W for Y39A was determined to be equal because even at high concentrations of IIA^{Glc} the enzyme was not found to be inhibited. The increase in the coupling factor, W, reiterates the importance of the domain I residue Y39 in IIA^{Glc} inhibition. The value of W is >1 if the allosteric effector increases the V_{max}, and is <1 if V_{max} is reduced by the allosteric effector. The alanine substitutions of the Y39 residue therefore appeared to decrease the ability of the EcGK enzyme to reduce the V_{max}.

To evaluate the role of the tyrosine hydroxyl group and aromatic ring in the loss of IIA^{Glc} inhibition of the Y39A variant, the Y39F variant was constructed. The increase in $K_{0.5}$ for the Y39F variant suggests that the hydroxyl group interaction of Y39 with Arg^{369} may still be important in IIA^{Glc} binding. The large effect of the Y39A substitution on IIA^{Glc} inhibition was therefore largely due to the loss of the interactions of the aromatic ring. The hydroxyl group interaction of Y39 with Arg^{369} however does not appear to be very important for inhibition since W for the Y39F variant was not significantly different from the Wild Type enzyme.

The W for the domain II bridging variants was not significantly different from Wild Type, suggesting that the alanine mutations at these sites did not affect the ability of the enzyme to reduce the V_{max} during IIA^{Glc} inhibition. The $K_{0.5}$ for IIA^{Glc} binding

also remained similar to Wild Type, indicating that the domain II alanine substitutions did not affect the affinity for the inhibitor. These results indicate that the domain II bridging interactions with Arg^{369} may not be important in regulating inhibition of the enzyme by IIA^{Glc}.

Since the analysis of the crystal structure of the EcGK by Hurley et al. (5) showed Arg^{369} as an acid residue likely to be important in the IIA^{Glc} regulation of EcGK, the crystal structures of two variant EcGK were superimposed in an attempt to illuminate any differences which may exist between the inhibited and uninhibited forms of the enzyme around the Arg^{369} residue. A previously determined crystal structure of EcGK with FBP bound was used to mimic the inhibited closed conformation of EcGK (40) and superposed with the structure of an EcGK variant S58W variant which is not inhibited by FBP (41). The crystal structure of the S58W variant of EcGK shows two asymmetric monomers in the dimer and the open form was used to mimic the uninhibited conformation of EcGK. The superimposed crystal structures shown in Figure 24 showed some differences in movement for the domain I amino acid residues within 4 Å which interact with the Arg^{369} loop. The domain II amino acid residues within 4 Å interacting with the Arg^{369} loop however do not seem affected by the open or closed conformations (Pettigrew, D.W unpublished). The observed movement of the domain I residues in close proximity to Arg^{369} is in agreement with the observed effects of domain I in regulating IIA^{Glc} binding to the enzyme.

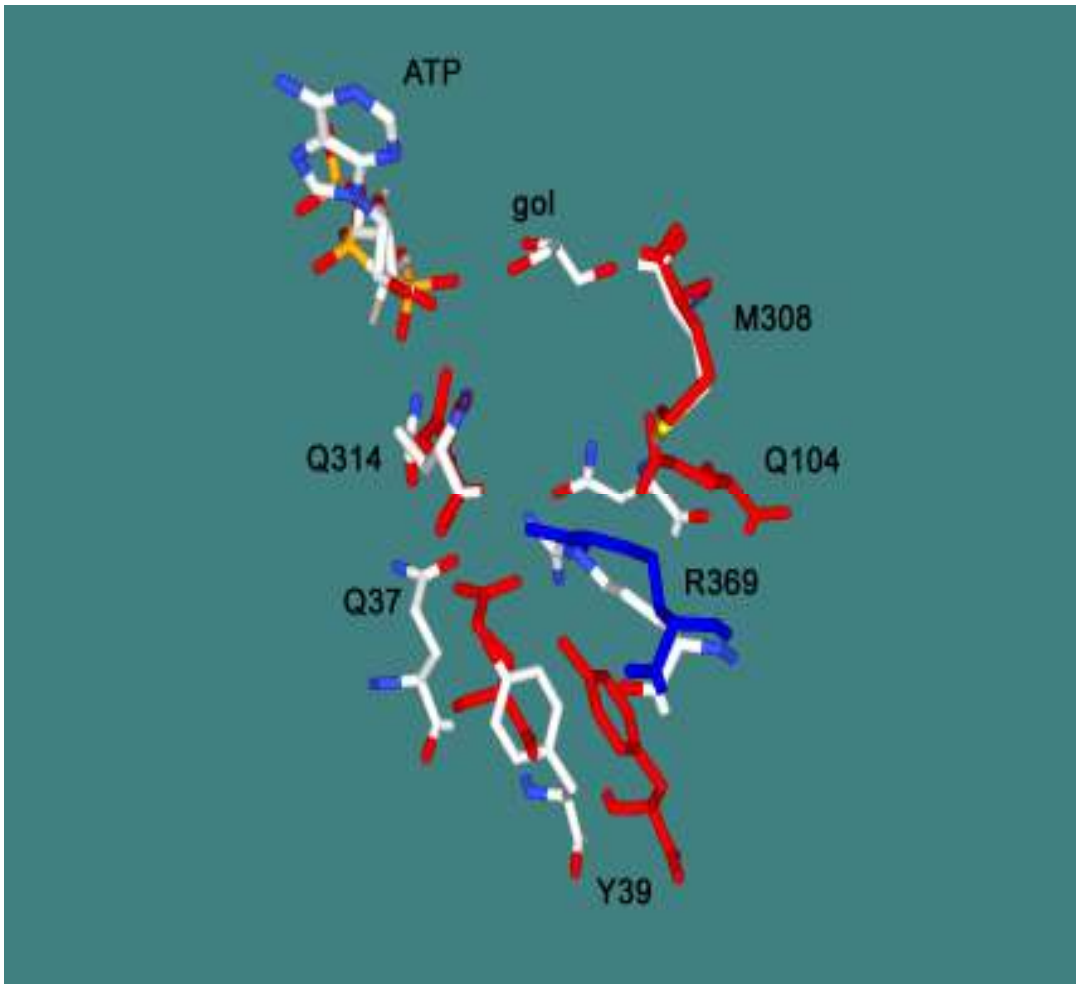

Solid color: EcGK·FBP complex (PDB: 1BO5). Inhibited closed conformation
CPK color: S58W·gol·ADPCF$_2$P complex (PDB: 1BWF). Open uninhibited conformation (asymmetric monomers in dimer)

Figure 24: Superimposed crystal structures of *E. coli* glycerol kinase. The superimposed structure is a composite of structures from pdb files 1BO5 (40) and 1BWF (41). The pictures were generated from the crystal structures of EcGK using PyMOL (generously performed by Dr. Pingwei Li of Texas A&M University) and the superposition done using Deep View/Swiss-PdbViewer version 3.7 (42) and POV-Ray version 3.1 (www.povray.org) by Dr. Donald Pettigrew of Texas A&M University.

Importance of the Domain Bridging Amino Acids in FBP Regulation of EcGK

Previous studies have suggested that FBP and IIA^{Glc} inhibition can be genetically separated. The effects of the R369A substitution which formed the basis of this study also indicated that the Arg^{369} residue was important only in IIA^{Glc} inhibition, but had no observable effects on FBP inhibition. Inhibition to EcGK by FBP for the domain bridging variants was therefore investigated to evaluate the importance of the domain bridging amino acids in FBP inhibition.

From Table 5, it can be seen that with the exception of Q104A, the domain I alanine substitutions resulted in significant increases in the $K_{0.5}$ for FBP binding. The apparent binding affinity for FBP therefore appeared to be reduced due to the alanine substitutions. The domain I residues Q37 and Y39 therefore appear important in regulating FBP binding to the enzyme. For Y39, the FBP parameters of the phenylalanine variant were used to assess the importance of the hydroxyl group interaction with R369 in FBP inhibition. From the results in Table 5 for the Y39F variant, the hydroxyl group interaction of Y39 with Arg^{369} appears important in FBP binding although to a lesser extent than the hydrophobic portion. This is because removal of the hydroxyl group interaction by the phenylalanine substitution still affected the affinity of the enzyme for FBP as seen by the increase in the $K_{0.5}$. The $K_{0.5}$ for FBP binding of the domain I variant Q104A was not affected by the alanine substitutions, suggesting that this residue does not play a significant role in FBP binding. The coupling parameter, W, was not affected by any of the amino acid substitutions of the domain

I bridging residues. The residues studied may therefore not be essential in regulating the V_{max} during FBP inhibition.

The domain II variant, M308A was interesting because the $K_{0.5}$ for FBP binding was lower than that of Wild Type. This observation suggests that the alanine substitution resulted in a variant which had a higher affinity for FBP. The implication of this for FBP binding is unclear. It is possible that the M308 residue is in the allosteric network for the regulation of FBP binding, and the interaction of M308 with Arg^{369} acts as a check to control the affinity of FBP binding. For the domain II substitutions, the $K_{0.5}$ for FBP binding of the Q314A was not affected by the alanine substitution. The Q314 interaction with Arg^{369} may therefore be unimportant in regulating FBP binding. The W for domain II variants, M308A and Q314A were not significantly different from that of Wild Type, suggesting that these residues may unimportant for inhibition of the enzyme by FBP. The Hill coefficient for all the domain bridging variants studied were greater than one, indicating that the amino acid substitutions did not affect the positive cooperativity of FBP binding to EcGK.

The observation that some domain I residues important for IIA^{Glc} inhibition were also important for FBP inhibition was interesting. This observation suggests that signals involved in IIA^{Glc} inhibition may go through channels which overlap the paths involved in FBP inhibition. Novotny et al, (18) and subsequently Saier (19) concluded that the regulation of FBP and IIA^{Glc} inhibition operates by independent mechanisms because: 1) Mutants have been isolated which lack one type of regulation but completely retain regulation by the other. 2) IIA^{Glc} inhibition of EcGK has not been found to be

concentration dependent but FBP inhibition of EcGK has been found to be concentration dependent. 3) The inhibitory effects of FBP and IIA^{Glc} have been found to be additive at subsaturating conditions. These results however suggest that the domain I bridging residues Q37 and Y39 may be important for both FBP and IIA^{Glc} inhibition.

The phenotypes of the variants on MGSA plates (displayed in Table 6) are also consistent with the kinetic results. Wild Type glycerol kinase is purple on MGSA. Cells which lose FBP control of glycerol kinase have been observed to have a foggy purple phenotype on MacConkey glycerol, due to the uncontrolled use of glycerol as a carbon source. The domain I variants had a foggy purple phenotype consistent with the higher $K_{0.5}$ values which are indicative of loss of FBP control. The M308A variant also had a pink phenotype consistent with the lower $K_{0.5}$ value which is indicative of more FBP control. The Q314A variant which had $K_{0.5}$ value similar to Wild Type was still purple.

Effects of the Domain Bridging Substitutions on the Catalytic Properties of EcGK

The Arg^{369} residue which penetrates from one subunit into another is found approximately 10 Å from the catalytic cleft of EcGK. The kinetic parameters V_{max} and K_m were therefore obtained for one of the substrates, ATP to assess the effects of the Arg^{369} domain bridging substitutions on the catalytic properties.

The alanine substitutions of the domain I residues Q37A, Y39A and Q104A affected the catalytic properties. The effect was however mild in Q37A, where the V_{max} was reduced by about 30% and the Michaelis constant was unaffected. This residue therefore appears to be important for catalysis, but not for substrate binding. The Q37A

substitution may have resulted in a local change in the enzyme which was not favorable for one of the chemical steps in the enzyme catalyzed reaction resulting in the observed reduction in the V_{max}. The major effect on the catalytic properties was observed for the domain I Y39A substitution. The V_{max} was substantially reduced by about 80% and the Michaelis constant increased about 12-fold. The large effects of this mutation on the catalytic properties were interesting because this residue appeared to be vital for IIA^{Glc} inhibition. The observed decrease in the V_{max} is suggestive that the interactions and/or local motions of the Y39 residue with Arg^{369} may be important in regulating the activity of the enzyme. The increase in the Michaelis constant also suggests that the Y39 residue is important in ATP binding.

Due to the large catalytic effects observed for the Y39A mutation, the second substrate, glycerol, was also varied in the assays to allow determination of the Michaelis constant for glycerol and the dissociation constant for ATP. The Michaelis constant and dissociation constants are displayed in Table 8. The results show that the Y39A mutation resulted in an increase in the Michaelis constant for both ATP and glycerol. In EcGK, it has been observed that the Michaelis constants for the substrates ATP and glycerol are about 5 to 10 fold smaller than the substrate dissociation constants. This observation suggests that a step after the formation of the ternary complexes may be rate limiting. The Y39A substitution however did not eliminate the difference between the Michaelis and dissociation constants for ATP. Unlike the Wild Type enzyme however, the Michaelis constant was about 2-fold larger than the dissociation constant for ATP. The Y39A substitution may therefore have resulted in a switch of the rate limiting step to

occur before the formation of the ternary complexes. The effects of the Y39A substitution on the catalytic properties of EcGK are somewhat similar. The V_{max} of the R369A variant was decreased similar to what was observed for Y39A. There was also a significant increase in the K_m for ATP and glycerol for both variants. The alanine of both residues also affected the K_m/K_{ia} ratio for ATP binding. These results therefore suggest that the interaction of Arg^{369} and Y39 may be important for regulating the formation of the ternary complexes during catalysis of EGK.

The phenylalanine variant of Y39 constructed to assess the hydrogen bonding interactions of the hydroxyl group on the tyrosine residue with Arg^{369} showed some interesting results. The Y39F substitution had very little effects on the catalytic properties of EcGK. There appeared to be no significant effect on the Michaelis constant, while the V_{max} was slightly increased approximately two-fold. The observed two-fold increase in the V_{max}, although small, may indicate an associated increase in the rate of motion of the interaction between Y39F and Arg^{369}. The hydroxyl group of Y39 may therefore be important in regulating the rate of motion in its interaction with the Arg^{369} residue but may not be vital during catalysis. The interactions of the hydrophobic portion of the tyrosine residue with Arg^{369} may therefore be more important in the enzyme catalysis since the alanine substitution reduced the area of the hydrophobic group interacting with Arg^{369}, with a resultant reduction in the V_{max} and an increase in the Michaelis constant.

For the third domain I variant, Q104A, the V_{max} appeared to increase almost two-fold, while the Michaelis constant increased about eight-fold compared to the Wild Type

enzyme. The Q104A substitution therefore appeared to result in a decrease of the binding affinity for ATP, but increased the catalytic rate. The interaction of this residue with the Arg^{369} residue may therefore be important for substrate binding, but not significantly important for catalysis. The increase in V_{max} observed may be due to a conformational change resulting from the alanine substitution of Q104 which was favorable for an increased the rate of catalysis of the enzyme.

With the domain II alanine substitutions, M308A and Q314A, only the M308A substitution affected the catalytic properties of the enzyme. The V_{max} and Michaelis constant of the Q314A variant were unaffected by the alanine substitution, suggesting that the interaction of this residue with Arg^{369} is not important in catalysis or substrate binding. The V_{max} of the M308A variant was however approximately 60% lower than that of Wild Type, but the Michaelis constant remained unaffected. This interaction of the M308A residue with Arg^{369} therefore appears important during catalysis of the enzyme. The different values of V_{max} seen for the EcGK variants may be related to different contributions of each residue interaction with Arg^{369} and the effect on the rate of the active site closure motion. For example, the Y39F substitution resulted in an increase in the V_{max}; apparently indicating an associated increase in the rate of motion at the active site.

The kinetic results indicate that the hydrogen bonding interactions of the domain I residues, Q37A and Y39A with the guanidino group of Arg^{369}, as well as that of the domain II residue M308A with Arg^{369} are important during catalysis. The interactions of the domain I residues however appear to be more important for substrate binding than the interactions of the domain II residues with Arg^{369}. Since these residues are far removed from the catalytic site of the enzyme, the results indicate that the domain I may form part of the network in communicating ATP binding to the active site during catalysis.

CHAPTER V

CONCLUSIONS

The results from this study indicate that the domain I bridging interactions with Arg^{369} are important in IIA^{Glc} regulation of the *E. coli* glycerol kinase enzyme. The domain II bridging interactions appear to be unimportant in regulating IIA^{Glc} inhibition. The domain I bridging residues Q37 and Y39 were also found to be important in FBP inhibition. From the observations of Novotny et al., (18), EcGK has the ability to genetically separate FBP and IIA^{Glc} inhibition. These results however indicate that some residues seen to be involved in IIA^{Glc} regulation also appear to be involved in FBP regulation. In catalysis, with the exception of Q314, the other domain bridging residues appear to be important for substrate binding and/or catalysis.

REFERENCES

1. Lin, E.C.C. (1976) *Annu. Rev. Microbiol*. **30,** 535-578

2. Phibbs, P.V. Jr., McCowen, S.M., Feary, T.W., and Blevins, W.T. (1978) *J. Bacteriol.* **133,** 717-728

3. Freedburg, W.C., and Lin, E.C.C. (1973) *J. Bacteriol.* **115,** 816-823

4. Miki, K., Silhavy, T.J., and Andrews, K.J. (1979) *J. Bacteriol.* **138,** 268-269

5. Hurley, J.H., Faber, H.R., Worthylake, D., Meadow, N.D., Roseman, S., Pettigrew, D.W., and Remington, S.J. (1993) *Science* **259,** 673–677

6. Anderson, C. M., Stenkampe, R.E., McDonald, R.C., and Steitz, T.A. (1978) *J. Mol. Biol* **123,** 207-209

7. Flaherty, K.M., Flaherty-DeLuca, C., and McKay, D.B. (1990) *Nature* **346,** 623-628

8. Kabsch, W., Mannherz, H.G., Suck, D., Pai, E.F., and Holmes, K.C. (1990) *Nature* **347,** 37-44

9. Bennett, W. S., and Steitz, T. A. (1980) *J. Mol. Biol.* **140,** 211-230

10. Hurley, J. H. (1996) *Annu. Rev. Biophys. Biomol. Struct.* **25,** 137-162

11. Grueninger, D., and Schulz, G. E. (2006) *J. Mol. Biol.* **359,** 787-797

12. Pettigrew, D. W., Yu, G.-J., and Liu, Y**.** (1990) *Biochemistry* **29,** 8620-8627

13. Voegele, R.T., Sweet, G.D., and Boos, W. (1993) *J. Bacteriol.* **175,** 1087-1094

14. Zwaig, N., and Lin, E.C.C. (1966) *Science* **153,** 755-757

15. Lin, E.C.C in: F.C. Neidhardt (Ed.), *Escherichia coli and Salmonella. Cellular and Molecular Biology*, ASM Press, Washington, DC, 1996, pp. 307–342

16. deRiel, J.K., and Paulus, H. (1978a) *Biochemistry* **24,** 5134-5140

17. Postma, P.W., Epstein, W., Schuitema, A., R., and Nelson, S.O. (1984) *J. Bacteriol.* **158** (1), 351-353

18. Novotny, M. J., Frederickson, W. L., Waygood, E. B., and Saier, M. H., Jr (1985) *J. Bacteriol.* **162,** 810-816

19. Saier, Jr. M.H. (1989) *Microbiol. Rev.* **53,** 109-120

20. Pettigrew D.W. (2009) *Arch. Biochem. Biophys.* **492,** 29-39

21. Swain, J. F., and Gierasch, L. M. (2006) *Curr. Opin. Struct. Biol.* **16,** 102-108

22. Kern, D., and Zuiderweg, E. R. P. (2003) *Curr. Opin. Struct. Biol.* **13,** 748-757

23. Monod, J., Wyman, J., and Changeux, J. (1965) *J. Mol. Biol.* **12,** 88-118

24. Koshland, D. E., Némethy, G., and Filmer, D. (1966) *Biochemistry* **5,** 365-385

25. Suel, G., Lockless, S., Wall, M., and Ranganathan, R. (2003) *Nature Struct. Biol.* **10,** 59–69

26. Yu, P., Lasagna, M., Pawlyk, A. C., Reinhart, G. D., and Pettigrew, D.W. (2007) *Biochemistry* **46,** 12355-12365

27. Goodey, N., and Benkovic, S. J. (2008) *Nat. Chem. Biol.* **4,** 474–482

28. Daily, M. D., Upadhyaya, T. J., and Gray, J.J. (2008) *Proteins* **71,** 455–466

29. Liu, W.Z., Faber, R., Feese, M., Remington, S.J., and Pettigrew, D.W. (1994) *Biochemistry* **33,** 10120-10126

30. Wüthrich, K. (1998) *Nature Struct. Biol.* **5,** 492-495

31. Pelton, J.G., Torchia, D.A, Meadow, N.D., Wong, C-Y., and Roseman, S. (1991) *Biochemistry* **30,** 10043-10057

32. Pettigrew, D. W., Ma, D.P., Conrad, C. A., and Johnson, J. R. (1988) *J. Biol. Chem.* **263,** 135-139

33. Stewart, G. S**.** A. B., Lubinsky-Mink, S., Jackson, C. G., Cassel, A., and Kuhn, J. (1986) *Plasmid* **15,** 172-181

34. Maniatis, T., Fritsch, E. F., and Sambrook, J. (1982) *Molecular Cloning: A Laboratory Manual 1.* Cold Spring Harbor Laboratory, Cold Spring Harber, NY

35. Pettigrew, D.W. (1986) *Biochemistry* **25,** 4711-4718

36. Pettigrew, D.W., Meadow, N.D., Roseman, S., and Remington, S.J. (1998) *Biochemistry* **37,** 4875–4883

37. Pawlyk, A., and Pettigrew, D.W. (2002) *Proc. Natl. Acad. Sci. U.S.A.***99,** 11115 – 11120

38. Garcia de la Torre, J. Huertas, M.L., and Carrasco, B. (2000) *Biophys. J.* **78,** 719-730

39. Pettigrew, D.W. (2009b) *Arch. Biochem. Biophys.* **492,** 29-39

40. Ormo, M., Bystrom, E.C., and Remington, S.J. (1998) *Biochemistry* **37,** 16565-16572

41. Bystrom, C.E., Pettigrew, D.W., Branchaud, B.P., O'Brien, P., and Remington, S.J. (1999) *Biochemistry* **38,** 3508-3518

42. N. Guex, M.C. Peitsch, *Electrophoresis* 18 (1997) 2714–2723

VITA

Name:	Edith Abena Acquaye
Address:	Department of Biochemistry and Biophysics, c/o Dr. Donald Pettigrew, Texas A&M University, College Station, TX, 77843-2128
Email Address:	acqu21@tamu.edu
Education:	B.Sc. Biochemistry, University of Ghana, Legon, 2006 M.S., Biochemistry/Biophysics, Texas A&M University, 2010